Using Big Data to Evaluate Traffic Signal Performance for the State of Tennessee

By

Piro Andruga Meleby

A Thesis Submitted in Partial Fulfillment of the Requirements for the Degree of Master of Science in Engineering Technology

Middle Tennessee State University

December 2022

Thesis committee:

Dr. Lei Miao, Chair

Dr. Saleh Sbenaty

Dr. Mina Mohebbi

Dedication

To my mother, Ms. Savia Sylvester, my father, Dr. Jino Meleby, my uncle and aunt Edward and Emilia Lado, for always being in my corner. You encouraged me to always continue pushing steadily, despite setbacks along the way.

ACKNOWLEDGEMENTS

I would like to thank my thesis advisor Dr. Lei Miao for continuously guiding me throughout the duration of this research. Without him, I would not have come thus far. I would like to thank undergraduate students Asma Mohammed & Tamir Hussein who helped implementing the webserver. Bill Leitzan of Southern Lighting and Traffic and Philip Blaiklock of Atkins extended their expansive expertise on the inner workings of the traffic signal controller and the ATSPM website respectively. Without them, much of the work done in simulating a functioning signaled intersection would not be possible, and for that I am very thankful. Lastly, I would like to thank Dwight Hutson and Brian Robinson, MTSU System Administrators who assisted in the hosting of the ATSPM website on the University server and making it accessible.

ABSTRACT

Congestion on roadways has led to increased travel time, waste of fuel, and higher emissions. Compared with other methods such as constructing more lanes and/or roads, traffic signal retiming is a viable alternative way to mitigate congestion. To prioritize retiming and to understand the impact of signal retiming, the performance of signals needs to be evaluated. This thesis details a data-driven and low-cost methodology funded by the Tennessee Department of Transportation for evaluating the performance of traffic signals in Tennessee using third-party segmented probe vehicle data. Intersections were formed by matching the names and geographical information of inbound segments. The average speed, the worst-case travel time, and the bottleneck ranking data during different times of the day for each segment at an intersection were used to develop metrics for a ranking formula that outputs a numerical value from 0-10 for each intersection. The results were appended to an online database accessible via a webpage with search and sorting capabilities. The ranking formula results were compared with the Level-of-Service ranking provided by local traffic engineers in the Cities of Murfreesboro and Franklin.

Additionally, testing was conducted on an industry-standard traffic signal controller for its data logging and networking functionalities. An Automated Traffic Signal Performance Measures (ATSPM) server and a website were also set up to display various performance measures of traffic signals. The traffic data was generated by emulating stop bar and advance loop detector events in a lab environment.

Contents

LIST OF FIGURES

LIST OF SYMBOLS/ABBREVIATIONS/TERMS

ATSPM	Automated Traffic Signal Performance Measures
GPS	Global Positioning System
LOS	Level of Service
PDA	Probe Data Analytics
PTI	Planning Time Index
RITIS	Regional Integrated Transportation Information System
TMC	Traffic Message Channel
TOD	Time of Day
XDs	eXtreme Definition Segments
MDD	Massive Data Downloader
SURTRAC	Scalable Urban Traffic Control
BRA	Bavarian Road Administration
IC	Integrated Circuit (board/chip)

Chapter 1 Introduction

The increase in the number of vehicles on roads has led to a rise in vehicular congestion, especially in areas with high/increasing population density. The national cost of congestion in the United States increased by approximately 500%, from $24 billion in 1982 to $121 billion in 2011 [1]. By 2011, the commuters are said to have collectively spent an additional 7.2 billion travel hours and burned an extra 3.1 billion gallons of fuel simply due to congestion. Since then, the trend of increasing congestion has continued, with 2019's pre-COVID-19 national congestion cost rising to $190 billion [2]. Commuters concurrently experience the effects of congestion first-hand, through increased travel times and diminished fuel economy. Governments experience reduced quality and efficiency of road utilities including poor emergency response, and increased frequency (and severity) of accidents. Whereas for commuters and the government the effects of congestion are experienced in the short-term, the environmental impact is far more gradual and much more challenging to remedy. It is estimated that 29% of all emissions in 2019 were attributed to the transportation sector, with more than half of that contributed by light-duty vehicles including passenger cars and light-duty trucks [3]. A sum of 36 million tons of greenhouse gases produced in 2019 were created due to congestion alone [2].

Hence it is important to mitigate congestion on roadways to minimize the economic and environmental impact. There is a bevy of ways to carry out congestion relief actions as illustrated in Figure 1-1 below. These actions can categorically be broken down into

limiting the number of vehicles on roadways and improving road capacity to handle the traffic demand.

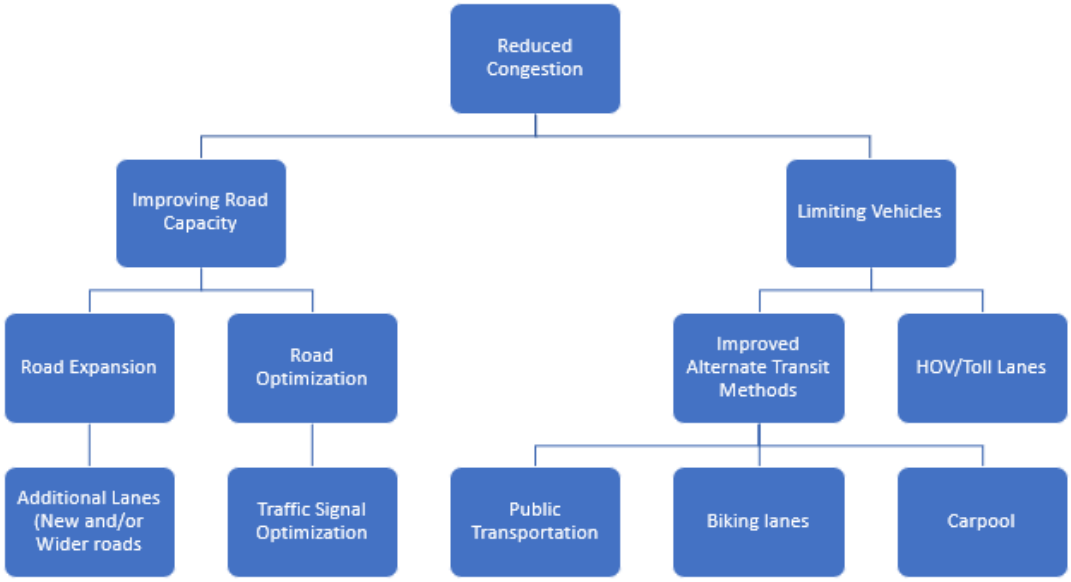

FIGURE 1-1 DICHOTOMY OF CONGESTION RELIEF MEASURES.

The former consists of measures to promote and improve alternate forms of transportation to reduce the dependence on private vehicles as the primary mode of transportation. These measures are founded on strong policy and commitment from commuters, as well as availability of resources to expand and maintain the alternate transportation modes. Many cities in Europe limit vehicles in busy city centers to allow for walkability and bicycle use, while countries like South Korea and Japan employ extensive networks of high-speed rail as efficient modes of transportation. Since these

undertakings aim to reduce the number of vehicles on the road, they garner more support where initiatives to reduce environmental pollution are in heavy consideration.

The alternative approach to fighting congestion focuses on road capacity, in which roads are either expanded for general use or optimized. Road expansion projects are often long and expensive endeavors for governments and end up causing congestion and bottlenecking along nearby roads and intersections due to limited lane availability and traffic detouring. Furthermore, it has been documented that road expansion projects do not significantly improve congestion, hence not completely justifying the investment [4]. Duranton et al. conducted a study based on the "fundamental law of highway congestion" [5], in which the law was expanded beyond highways onto major roads [6]. Their findings suggested that increasing road capacity is not an appropriate approach to tackle congestion. Additional studies [7, 8] reached similar conclusions, with the latter suggesting road pricing as an alternative solution to congestion. However, congestion pricing projects like the introduction of toll lanes do not receive massive or sustained support from the public [9, 10, 11]. These methods often require any combination of significant investment from the government, policy changes and public support, a significant change in the commuting patterns of the public and additional travel costs.

Road optimization projects are less intrusive to drivers due to the utilization of already existing infrastructure and at no significant cost to the driver, hence garnering greater support [12]. Some solutions include the use of alternate lanes to increase the flow of traffic in the congested direction while operations including optimization of traffic signals performance are more complex. There are more than 272,000 traffic signals in the

U.S. alone, and traffic signal retiming is one of the most cost-effective ways to improve traffic flow and mitigate congestion [13]. Each state or local transportation agency in the United States has a considerable number of traffic signals under its purview, and many of these agencies do not have a framework through which signal performance is analyzed to directly impact retiming efforts [14, 15]. Instead, these agencies rely on citizens' complaints to respond to congestion at specific intersections, and random periodic schedules of up to five years to retime traffic signals, instead of the recommended two years. These methods are slow for the former, and highly ineffective and irregular for the latter. In both cases, poorly performing signals are not correctly identified, and the agencies do not have said signal performance evaluation framework to evaluate the performance after retiming efforts. Such a framework requires large quantities of data to capture the real traffic conditions on the roads. Signal performance data is time-based and includes mostly speed and travel time-related measures. Traffic technicians and engineers can also glean many more performance measures from the placement of sensor equipment at/near an intersection. These measures are used to evaluate performance and prioritize retiming of signals at poorly performing intersections for continuous improvement as shown in the process flow in Figure 1-2 below.

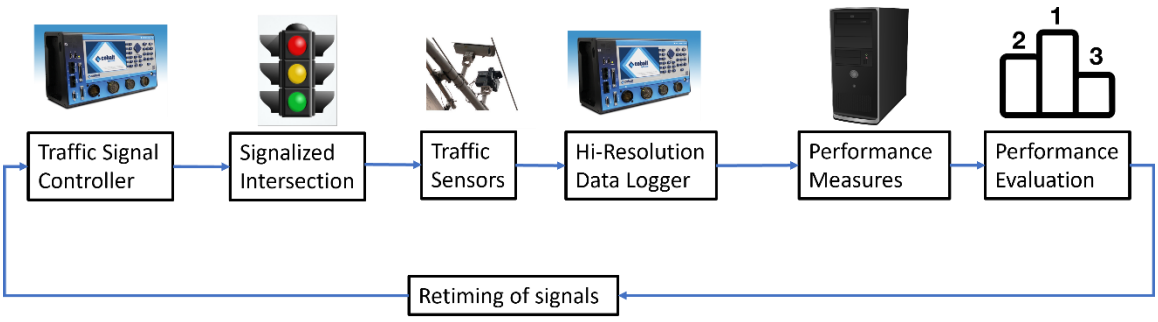

FIGURE 1-2 PROCESS FLOW FOR TRAFFIC SIGNAL RETIMING

In this system, the traffic signal controller, which is discussed later in this thesis, serves as the "brain" of a signalized intersection. Timing sequences are fed into it to control traffic flow and connected data collection hardware including detectors and cameras feed it detection results which are then timestamped. Performance measures are then compiled, and signals are compared to others to determine relative performance. This process is data intensive and requires ample computing power and storage, so it is important for transportation agencies to have the required infrastructure to carry out these operations effectively and efficiently.

The crux of the matter then becomes the availability of resources to firmly establish these operations. There are different data sources and methodologies that are implemented to evaluate performance of traffic signals. Some of the data sources include sensors equipment installed at intersections, probe vehicle data and probe vehicle trajectory data, as well as simulations and machine learning. Probe vehicle trajectory data, simulations and machine learning are emerging technologies and have not been widely utilized in comparison to sensors and probe vehicle data. A review of the studies conducted using these data sources was conducted and presented by the author in a journal [16].

Figure 1-2 summarizes the process of performance evaluations of traffic signals using traffic sensors for continuous improvement. It shows a high-level map for the ATSPM system where this setup of sensors is replicated at hundreds of intersections across a state, and data is gathered and processed in an online server and displayed on a browser Utah ATSPM. A similar system, the Freeway and Arterial System of Transportation (FAST), has been implemented in the state of Nevada. Such systems require a large network of sensors and camera equipment which can be quite expensive for local/regional traffic agencies. The

systems are also designed such that a commuter can view near-real time traffic conditions on the web interface, so data is continuously being drawn from the sensors and traffic controllers. This requires extensive storage both for processing in the short term, as well as for studies utilizing historical data in the long term. The implementation and management of such systems becomes an expensive endeavor overall thus many state transportation agencies have not implemented ATSPM. Therefore, it is important to develop alternate cost-effective methods to evaluate signal performance and allow for agencies to make well-informed decisions based on field data.

The work detailed in this thesis considers one such method, using probe vehicle data to develop a ranking system on a scale of 0-10. The method utilizes average speed and travel time-based measures for traffic signals in Tennessee to help agencies prioritize retiming. The results will be made available internally for the agencies, with a web interface for the public to view intersection rankings. In Chapter 2, some of evaluation methods in which probe vehicle data was utilized were detailed. In Chapter 3, the methodology on which this thesis is based is introduced. This chapter covers how the initial probe vehicle data was processed to provide a list of intersections using the identifier information, as well as how the ranking metrics and formula were developed. In Chapter 4, the results and their implications were discussed. Chapter 5 presents some initial testing of a Cobalt traffic signal controller capability, and a demonstration of the ATSPM system using the controller and a configuration of detectors simulating calls into the controller. Chapter 6 covers the conclusion of the thesis and an outlook for this field of research.

Chapter 2 Literature Review

Probe vehicle data has been increasingly utilized by agencies and researchers alike to develop performance evaluation frameworks. These frameworks have utilized data analysis methods including metrics for both rankings, and graphical representations of evaluation results.

Rankings

Remias et al. performed four case studies to test the effectiveness of four different data collection methods for traffic signal performance evaluation [17]. The methods included agency-driven probe vehicles, re-identification with pavement sensors that can detect a vehicle's magnetic fingerprint, re-identification with Metropolitan Affairs Coalition address matching using Bluetooth Monitoring Station (BMS) scanners, and crowd-sourced data (commercial probe vehicle data from INRIX). The probe vehicle data was used to study the effect of retiming on travel time of two approaches along the corridor of study. Improvements in travel times were observed using the probe vehicle data. The overall results of the study were summarized in a table showing that crowd-sourced data had the best scalability, despite having a relatively smaller sample size.

Khattak et al. used travel time runs and INRIX probe vehicle data to obtain performance measures for scalable urban traffic control (SURTRAC) intersections in Pittsburg, Pennsylvania [18]. First, GPS floating car data was collected for different windows and travel time and speed measures were developed and evaluated for improvements. Considering the free flow travel time as the posted speed along a TMC segment, the planning time index was developed from the INRIX probe vehicle data:

$$\text{Planning Time Index (PTI)} = \frac{95^{th}\ \text{Percentile travel time}}{\text{free flow travel time}}$$

Bayesian linear regression models and volatility were also used to analyze performance before and after adaptive traffic control. Volatility was used to capture the 3-D movement of vehicles and other erratic movements that cause safety risks and efficiencies related to fuel use and emissions. The adaptive control was determined to have a net positive impact on speed, travel time, travel time reliability and planning time index. The probe vehicle data was also determined to consistently record longer travel times than the GPS data, but the changes in travel time were consistent for both data sets.

Day et al. [19] presents a methodology for analyzing and ranking arterial travel times. The analysis was performed on a series of 28 arterials with a total of 341 signalized intersections in Indiana, USA. The data consisted of individual minute by minute speed records which were then converted into travel times. To mitigate the effects from occasionally missing data, the speed records were pooled into 15-minute bins, and the average of the bins was used as the measured travel time in each segment for that period. Additionally, the authors divided a typical day into three intervals: morning peak (06:00-09:00), midday (09:00-15:00), and evening peak (15:00-19:00). T was used to denote the length of such an interval. Since the arterials varied in length and speed limits, two normalization methods were used on the data: *(i)* calculating travel rate r_T and *(ii)* calculating the ideal speed normalized travel time $x_T^{'}$ by dividing the average measured travel time by the ideal travel time. The travel rate r_T is the ratio of the average travel time over the distance of the corridor, effectively the reciprocal of the average speed. The

ideal speed normalized travel time is calculated as ratio of the average travel time to the speed limit travel time. Since r_T is dependent on the length of the arterial, $x_T^{'}$ serves as a better performance measure because it compares the average measured travel time to the travel time at the speed limit irrespective of arterial length. Additionally, the normalized reliability of travel time $s_T^{'}$, which the ratio between the standard deviation of the actual travel time and the speed limit travel time, was calculated. Finally, the arterial prioritization index was summarized in a formula:

$$\text{index}_T = 100 \cdot \sqrt{(\max\{0, x_T^{'} - 1\}^2 + (w \cdot s_T^{'})^2)},$$

where w is a weighting factor.

Data from several intersections was used to this study and their indices for the three TODs were compiled into one composite value. The intersections with higher composite indices were to be prioritized for retiming.

Dunn et al. used segmented probe vehicle speed data to rank the performance of 1,026 traffic signals along 79 corridors maintained by the City of Austin, Texas for retiming purposes [20]. The data used by this study was purchased by the City of Austin from a third-party vendor, which had a data set that covered 87% of the area of study. The data provided listed the average vehicle speed over segments of the road, with one minute speed averages. The data was downloaded from the provider and stored in a PostgreSQL database for use. The speed data was aggregated into 15-minute bins in TOD periods: morning peak (07:00-09:00), midday (11:00-13:00), and evening peak (16:00-18:00). There were three metrics used in the ranking process: the percentage of the corridor that

experienced any slowdown, the percentage of the corridor that experienced a slowdown greater than 3mph, and the maximum slow-down among all the segments for any given corridor. The final ranking was based on the average of rankings across the three TODs and the priority corridors were ranked higher than others. While this study evaluated involved the evaluation of corridors consisting of multiple intersections, rather than individual intersections, it highlighted the need to an evaluation methodology: out of 27 corridors that had been retimed by the City of Austin prior to this study, only 7 were near the top of the rankings, while 16 were much further down in the rankings. Based on the ranking formula, the City of Austin carried out more than half of its retiming efforts along corridors that were of lower priority.

Meijer et al. [21] used consumer vehicle GPS data provided by the floating car database from TomTom to measure delay and turning movements at intersections in the Dutch city of Delft. The authors utilized a multi-source multi-destination Dijkstra algorithm to analyze each individual measurement and link it to the most probable location on the road based on the chosen route of the vehicle. For measurement of turning movements, the results of the vehicles' GPS data were compared with a ground truth reference obtained by loop detectors and shown to be accurate with less than 3.8% error. When measuring delay, which was defined as the difference between uninterrupted and interrupted travel times through the intersection, the results from the GPS data were compared with those from the combination of loop detectors and a time-dependent stochastic delay model. In this case, there was no ground truth reference, and the two methods provided distributions with similar trend but deviations as large as 20 seconds during rush hour and nighttime periods. The authors proposed that the insufficient amount of GPS sample data

contributed to the discrepancy.

Wünsch et al. [22] used anonymous GPS probe data from navigation devices to perform a large-scale generic analysis for the Bavarian Road Administration (BRA) in Germany. The data provided was used to determine delay times and path-specific travel times for road segments that contained 2,300 traffic signals. Once the data was mapped to the corresponding intersections and reference travel times were determined using free-flow speed, the key performance indexes were calculated and used to rank the intersections. The metrics used were the delay per vehicle, total sample delay, and the travel time index. The total sample delay was defined as the summation of all measurements of the difference between measured travel time and the reference/free flow travel time. The delay per vehicle is the total sample delay divided by the number of measurements. Travel time index is the ratio of the observed travel times over the free-flow speed travel times. This study noted the influence of construction or road work near intersections, on the travel time measured by the GPS data. This leads to anomalies in the data collected and can skew any the evaluation results of those intersections.

The Pennsylvania Department of Transportation sponsored a study [23] to create a web dashboard interface that uses commercial probe vehicle data from INRIX to rank the performance of 138 corridors in Pennsylvania. The corridors were evaluated in terms of travel time, reliability, delay, and congestion based on segmented probe vehicle data. The data was collected from a web Application Programming Interface (API) via windows service program and automatically stored in a SQL database. Over the course of one year, roughly 30 billion data records were recorded. Using aggregated data across 15-minute

time intervals, travel time was calculated using a normalized median speed for a given road segment. The interquartile range was used as a measurement of reliability. Delay and congestion were measured using a plot showing a color-coded breakdown of a corridor based on the operating speeds for each section.

Graphical Analysis Methods

Cheng [24] worked with the Department of Transportation (DOT) of the City of Austin, Texas to develop and implement performance metrics to evaluate traffic signal effectiveness. Along with a modified corridor travel time, which the DOT was already using in evaluation, a few other metrics were developed including corridor travel time change, corridor throughput, side street split failures, pedestrian delay, transit speed change/transit ridership change, and reliability index change. Split failures occur when a vehicle needs to wait more than once cycle to traffic lights to get though an intersection. Most data used to obtain these metrics originated from Metric Blvd. because it was the only corridor that had recently been retimed. The graphical analysis was done on data from both before and after the retiming occurred. To investigate side street split failures, Kimley-Horn's online dashboard and aggregate report function were used for all intersecting corridors to Metric Blvd. The before and after graphs showed a decrease in total split failures on Metric Blvd. but the side corridors did not show a significant increase. INRIX data was used to determine the reliability index and was found to show an overall increase during peak hours. Using the data available through INRIX, a list of recommended corridors to be retimed for the next year was presented.

As determined by these studies, several issues plague the increased implementation of TMC segments. Chief among those are the low penetration rates and lack of uniformity

in segmentation leading to poor identification of signals. eXtreme Definition segments (XDs) have been developed to mitigate this issue. These segments are proprietary to INRIX and provide better signal identification and isolation than ordinary TMC segments. While these XD segments do not cover an overall area as wide as the regular TMC segments, their functional advantage has been utilized in multiple studies. A recent work that takes advantage of these XDs data to evaluate the effectiveness of adaptive traffic signal control in Des Moines, Iowa and Omaha, Nebraska, USA was conducted by Sharma et al. [25]. The researchers used raw vehicle speed data to generate cumulative distribution plots of speed, travel time, and then travel rate. Using the cumulative distribution plot of travel rate and a 90% confidence interval, the authors were able to classify all the days into two categories: typical and anomalous ones. The number of anomalous days per year was used as a metric to describe the travel time reliability of a segment. For normal days, the authors used five metrics to rank each segment. The first two were directly derived from the cumulative distribution plots: (i) Median travel rate, defined as the 50th percentile of the median of each day's travel rate and (ii) Within-day variability, defined as the median of the 95th percentile and the 5th percentile of a segment's travel rate. The other three were minimum travel rate dispersion, overall travel rate variability polynomial, and overall travel rate variability linear. These three were parameter coefficients obtained through curve fitting, which was done between the 90% confidence interval and the percentiles from 0% to 100%. In the case studies, the authors further classified the segments into 8 categories based on intersection density, which is defined as the number of intersections per segment, and the Annual Average Daily Traffic (AADT) per lane volume of the segment. Color-coded spider and bar plots were

used to show the performance of the segments based on the five metrics for each category. Some signals were observed to be under performing and one was selected to test adaptive signal control, resulting in small positive changes.

Brenna and Venigalla also experimented on the use of XD segment data by fusing high-resolution data from traffic signal systems and probe vehicle data [26]. Performance measures studied include probe vehicle speed and travel time to assess signal performance and data availability, and it was observed that minor changes in signal timing plans improve operational efficiencies of corridors.

Summary

Probe vehicle data provides a widely available and fiscally viable option for agencies because no heavy investment is needed for purchase and installation of a wide network of sensors and traffic controllers. This makes probe vehicle data a powerful tool for in-depth analysis of traffic performance and the development of novel evaluation methods. Probe vehicle data, either from commercial companies or crowdsourcing, has become increasingly popular in the past decade, due to technological advances in smartphones, GPS, and embedded systems. However, the granularity problem of the segments makes it hard to evaluate performance at each individual intersection; as a result, most works utilizing segmented probe vehicle data focused on the performance of arterials instead. Specifically, some TMC segments are much longer than others and these segments may have multiple signalized intersections along their lengths. This limits the identification of intersections because there are effectively no segments at the encompassed intersections, and no representative speed and travel time data. This has been alleviated by the

emergence of new types of segments such as the INRIX XDs, which over more miles of road, are more flexible, and offer higher granularity than the TMC segments. XD segments are proprietary and the additional expense in choosing to utilize them over TMC segments is not feasible for many resource-strapped agencies, hence limiting its widespread application.

Most of the studies reviewed in this thesis considered few performance measures to evaluate individual intersections and traffic control systems. While they documented mostly positive results when coupled with retiming actions, the measures used may be insufficient to determine a true comprehensive measure of the performance at an intersection. Most of the works reviewed evaluate the performance of either individual intersections or individual corridors with multiple major intersections. The work detailed in this thesis seeks to expand on this base of knowledge as follows:

1. Utilize segmented probe vehicle data to evaluate signal performance in an entire state.

2. Use the segments' geographical and identifier data to form the intersections regardless of segment length.

3. Develop metrics from the speed and travel time data for each segment and use the segment metrics to determine the signal performance. The metrics are to be compiled to provide a final signal rank on a scale from 0-10, with 10 being the best.

4. Present the ranking results in an online database to enable the storage of multiple iterations of performance evaluations using different sets of data.

5. Display the ranking results on a website accessed through a browser. The website reads from the database and displays the results with search and sort functionalities.

6. Test the working principle of a standard traffic controller to perform timing and receive detection calls to simulate a functioning field intersection.

7. Connect an ATSPM server and website to periodically receive traffic data from the simulated intersection and display relevant graphical performance measures.

This work seeks to be useful for traffic agencies and traffic researchers alike. To the best of the author's knowledge, such a concerted effort has not been documented and this work will provide great value to the current field of research.

Chapter 3 Methodology

Overview

The data used in this study was obtained from RITIS (ritis.org). Various streams of data including signal data, accident and repair data are integrated into RITIS. Probe vehicle data, provided by INRIX is also integrated into the website and is viewed through the Probe Data Analytics (PDA) Suite. INRIX presents the probe vehicle data in the TMC standard which covered many major roads in the state of Tennessee. In this study, the segments on interstate highways were excluded through a selection process before the data was delivered. Obtained through the Massive Data Downloader (MDD) in the PDA suite, the data was delivered as two comma-separated values (csv) files, *TMC Identification* and *Readings*. The former contained the geographical identifying information for TMC segments including road names, GPS coordinates, county, and zip code. The latter contained the probe vehicle readings obtained along the TMC segments including speed and travel time. A third csv file was also delivered for the bottleneck ranking and was used to develop the bottleneck ranking metric as explained later in this thesis. The data in all the files was invaluable in the process of determining intersection rankings. Figure 3-1 below provides a summary of this process.

FIGURE 3-1 PROCESS FLOW EMPLOYED FOR INTERSECTION RANKINGS

Intersection Extraction

The TMC standard is such that each direction of travel along a road has its own segment. An ideal T-junction intersection would be formed where six segments meet (share GPS coordinates), with three inbound and three outbound segments. Similarly, a crossroad intersection would be formed where eight segments meet with one half of the segments inbound and the other outbound. Segments have starting GPS coordinates at an intersection when the direction of travel is outbound and ending coordinates when the direction of travel is inbound. Figure 3-2 below shows a snapshot of the TMC identification file with the major identifiers for each segment.

	A	B	C	D	E	F	G	H	I	J	K	L
1	tmc	road	direction	intersection	state	county	zip	start_latitude	start_longitude	end_latitude	end_longitude	miles
2	121N50401	W 5TH AVE NW	WESTBOUND	US-441/BROADWAY NW	TN	KNOX	37917	35.97247	-83.92316	35.97251	-83.92395	0.044255
3	121N50402	W 5TH AVE NW	WESTBOUND	HALL OF FAME DR NE	TN	KNOX	37917	35.97576	-83.91677	35.976	-83.91823	0.084715
4	121N50404	E MAGNOLIA AVE NE	WESTBOUND	N CENTRAL ST	TN	KNOX	37917	35.97305	-83.9194	35.9726	-83.92011	0.050417
5	121N50405	US-11	WESTBOUND	HALL OF FAME DR NE	TN	KNOX	37917	35.97462	-83.91653	35.9745	-83.91707	0.031306
6	121N50407	TN-431	SOUTHBOUND	TN-431/UNIVERSITY ST	TN	WEAKLEY	38237	36.35348	-88.88638	36.35358	-88.88577	0.035131

FIGURE 3-2 SNAPSHOT OF THE TMC IDENTIFICATION FILE WITH MAJOR IDENTIFIERS.

Using nested loops in Python 3.1, a script was written to focus on the GPS coordinates provided for each segment. Each row in the TMC Identification file was read in the primary loop, and the end latitude and end longitude column values recorded. A nested loop looked at all *other* rows and compared the end latitude and end longitude values to find an exact match. The segment codes for matches were recorded in a list which was written to a text file after each iteration. Using only the data from inbound segments ensured that each intersection was ranked using data relevant to it and its effect would not be duplicated at other intersections upstream or downstream.

To determine the viability of the python script results, the *Trend Map* tool from the PDA Suite was used to visually very intersections. The tool allows users to enter specific TMC

codes and shows them on a map. Users can also draw geometrical figures on the map, and it returns all segments within its borders. To test the accuracy of the intersections extracted, random lists in the text file were copied and inserted into the Trend Map tool. Figure 3-3, 4 show samples of a T-junction and a crossroad intersection in the Trend Map, obtained from the initial group.

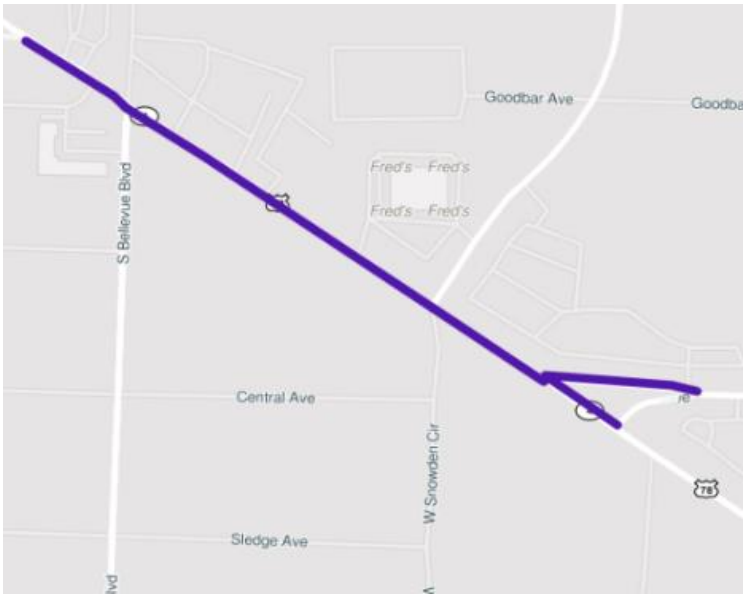

FIGURE 3-3 AN 'IDEAL' T-INTERSECTION FORMED AT CENTRAL AVE. AND TN-78 USING ONLY THREE INBOUND SEGMENTS.

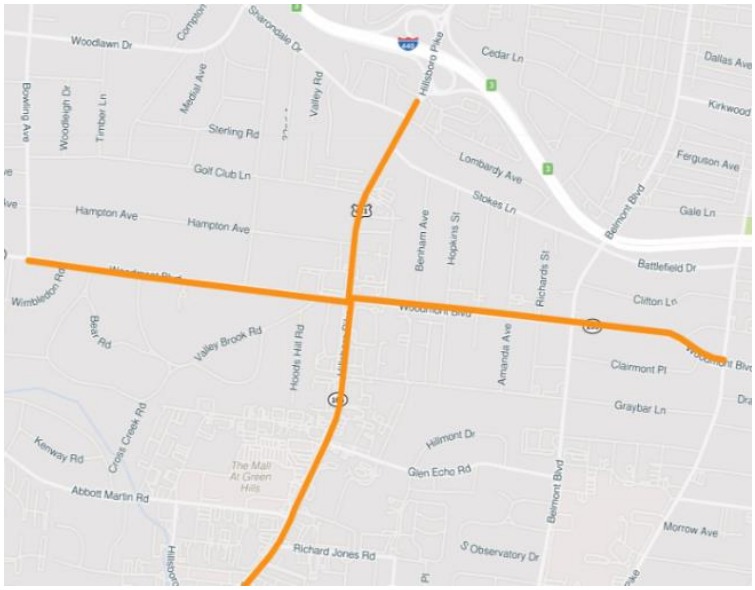

FIGURE 3-4 AN IDEAL CROSS-INTERSECTION FORMED AT HILLSBORO PK. AND WOODMONT BLVD. WITH FOUR INBOUND SEGMENTS.

Initially, only the ideal intersections as pictured (3 or 4 segments only) above were considered but their count did not reach 1000. It was imperative to further process the intersection the TMC Identification file to extract more intersections. In a new Python script, the list of intersections was expanded to include *all* 'intersections' where more than one segment had the same end coordinates and were written to one text file. Each line in the file contained a group of segments with their respective road and intersection names pooled together in a list at the end of the line. The names for each group of segments were extracted and compared to the names for all other groups of segments to find a match. A diameter of 50m was used as a secondary filter to only match the groups in proximity. The diameter was applied to the end coordinates of the segment pairs. These hybrid intersections were appended to the original list. Figures 3-5, 6 show two intersections, one formed as a combination of multiple pairs of segments ending at

different coordinates yet being part of the same intersection, and the other formed using only two inbound segments.

FIGURE 3-5 COMPLEX CROSS-INTERSECTION FORMED USING EIGHT PAIRS OF SEGMENTS AT TN-104 AND US-51 BYP.

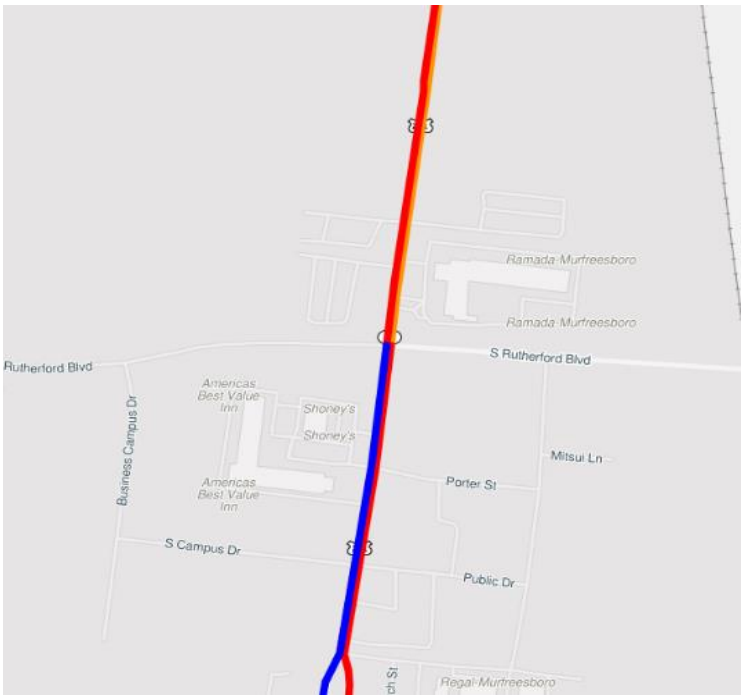

FIGURE 3-6 CROSS-INTERSECTION FORMED USING ONLY 2 INBOUND SEGMENTS AT RUTHERFORD BLVD. AND US-231.

The road names included all the alternate names for the segments that had more than one value in the intersection column. An intersection constituting the segment 121N50401 in Figure 3-7, would have the names W 5TH AVE NW, US-441 and BROADWAY NW' all recorded including road names from other segments at the intersection if they were not a match for the previous three.

tmc	road	direction	intersection
121N50401	W 5TH AVE NW	WESTBOU	US-441/BROADWAY NW
121N50402	W 5TH AVE NW	WESTBOU	HALL OF FAME DR NE

FIGURE 3-7 CLOSEUP OF THE TMC IDENTIFICATION FILE SHOWING DIVERSITY OF ROAD NAME VALUES FOR SOME SEGMENTS.

The total tally for the intersections rose to over 10,000 but given the nature of the segmentation, which will be further discussed later in this thesis, many of those were

found to be unviable through the Trend Map tool. A manual verification process yielded 1655 signalized intersections.

Ranking Formula

The ranking formula used three metrics to determine a rank, from 0-10, for all individual TMC segments. The rank for each intersection was then determined by averaging the ranks of the constituent TMC segments. The metrics used included congestion, Planning Time Index (PTI) and bottleneck ranking. The congestion was calculated using the average speed along the segment and hence represented the average traffic pattern along the segment, while the planning time index considered the near worst-case travel time at the 95th percentile. The bottleneck ranking shows the 1000 worst cumulative congestion locations over an extended period. The rank for each segment, R, is shown as a numerical value from 0-10, with 0 being the worst and 10 being the best.

$$R = w_p * R_p + w_c * R_c + w_b * R_b.$$

where:

- $R_p, R_c, and\ R_b$ are the contributing factors for planning time index, congestion, and bottleneck ranking, respectively. These performance metrics will be explained later in details.
- $w_p = 4.13, w_c = 4.62, and\ w_b = 1.25$ are weights assigned for planning time index, congestion, and bottleneck ranking, respectively. These weighting factors are crucial because their values affect the ranking results. The weight selection process is detailed in another concurrent work [27].

A *Readings* file that contains probe vehicle data for the 15,007 segments in Tennessee for every day in the entire month of September 2021 was created. Speed and travel time data for the segments averaged over five minutes for three three-hour (time-of-day) windows during the day to represent the time of the day in which traffic is dense: 6AM-9AM for morning, 11AM-2PM for midday and 4PM-7PM for evening. The first two hours in each time-of-day window were considered for weekdays and the last two hours are used for weekends. In a Python script, the Readings file was processed to produce the planning time index and congestion metrics.

Planning Time Index

The Planning Time Index (PTI) is defined as the total travel time that should be planned when an adequate buffer time is included. It compares near worst-case travel time to a travel time in light or free-flow traffic. It is calculated as the ratio of the 95^{th} percentile value of the travel time and the free-flow travel time.

In the Python script, a loop was initialized to look at each TMC segment and find and write to a list, the indices of all the times that the segment occurs in the Readings file. This list was then used to initialize a nested loop that scanned the timestamp column to determine the date and time of day of each occurrence using the *datetime* Python library. For all the occurrences in the morning, the travel time was appended to one list for weekdays and a second list for weekends. The free-flow travel time was determined by dividing the distance of the segment, read from the TMC Identification file, by the reference (free flow) speed of the segment and the time converted to seconds. The morning planning time index for that segment during weekdays and weekends was

calculated by dividing the 95th percentile value of each list by the reference speed travel time. The morning planning time index, P_1, given by

$$P_1 = \varepsilon_1 * P_{1,wd} + \varepsilon_2 * P_{1,we}.$$

where:

- $P_{1,wd}$ is the planning time index for the weekday morning and $P_{1,we}$ is the planning time index for the weekend morning.
- ε_1 and ε_2 are the weekday and weekend weighting factors, respectively.

Although the study covers all days of the week, much greater weights are assigned to weekdays than weekends due to the difference in number of days in weekdays and weekends, and the sheer volume of traffic experienced by each group. After consultation with the traffic department of City of Murfreesboro, it was determined that $\varepsilon_1 = 0.9$ and $\varepsilon_2 = 0.1$ would be appropriate weights. Many other studies only considered weekdays.

Planning time indices for the midday period, P_2, and the evening period, P_3, were calculated similarly. The aggregate planning time index, P_m, for each segment was then computed as

$$P_m = \alpha_1 * P_1 + \alpha_2 * P_2 + \alpha_3 * P_3.$$

Where α_1, α_2 and α_3 are the weighting factors for the three two-hour windows in the day. Likewise, greater weights were assigned to the morning and evening time-of-day windows than midday because the traffic volume is higher during rush hours: $\alpha_1 = 0.4$, $\alpha_2 = 0.2$ and $\alpha_3 = 0.4$.

A histogram of the values for P_m for all the TMC segments is plotted, as shown in Figure 3-8.

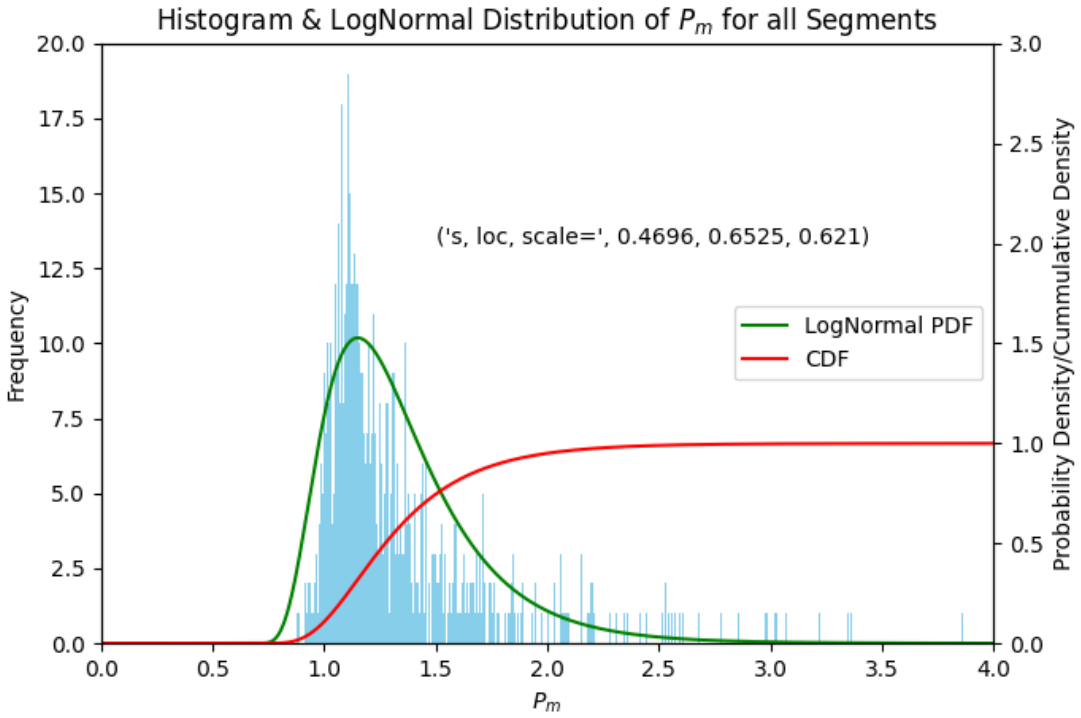

FIGURE 3-8 HISTOGRAM OF PM, THE FITTED APPROXIMATIONS OF A LOGNORMAL PROBABILITY & CUMULATIVE DISTRIBUTION FUNCTIONS.

From the histogram, the distribution of the PTI is approximated to a Lognormal distribution function. The value of R_p for a TMC segment is calculated using the cumulative distribution function $F_p(x)$ for a lognormal distribution, derived from the probability distribution function below.

$$f(x) = \frac{e^{-\left(\frac{\left(\ln\left(\frac{x-\theta}{\mu}\right)\right)^2}{2\sigma^2}\right)}}{(x-\theta)\sigma\sqrt{2\pi}}$$

$$R_p(P_m) = \left(1 - \left(\int_{-\infty}^{P_m} \frac{e^{-\left(\frac{P_m{}^2}{2}\right)}}{\sqrt{2\pi}}\, dt\right) * \left(\frac{\ln(P_m)}{\sigma}\right)\right)$$

where σ, θ and μ are the shape parameter and the location parameter and the scale parameter. In Figure 3-8 above, they are presented as *s*, *loc* and *scale* respectively.

Congestion

Congestion is a ratio of the measured speed to the free-flow speed, and it is closely related to travel time index, the ratio of average travel time to free-flow travel time. Free flow speed is defined as the calculated "free flow" mean speed for the roadway segment in miles per hour. This attribute, formerly calculated as the 85th percentile prior to March 2020, has since then been calculated as the 66th-percentile point of the observed speeds on that segment for all time periods. This establishes a reliable proxy for the speed of traffic at free flow for each segment.

The congestion was calculated in the same Python script loops as the planning time index, with a slight variation. The average speed values for each day were recorded in three separate lists for the morning, midday, and evening time-of-day windows. Averages were determined for each list and divided by the free flow speed to give congestion values C_1, C_2 and C_3, for the time windows, respectively. The aggregate daily congestion value, C_d, for one segment was calculated as

$$C_d = \alpha_1 * C_1 + \alpha_2 * C_2 + \alpha_3 * C_3\,,$$

where $C_1, C_2, and\ C_3$ are average congestion values for the three two-hour time windows.

The C_d values for each day were then stored in two lists, one for weekdays and the other for weekends. The averages for each list, C_{wd} and C_{we} respectively were calculated and the overall congestion for the TMC segment, C_m, is shown below, and a histogram of C_m values is plotted as in Figure 3-9.

$$C_m = \varepsilon_1 * C_{wd} + \varepsilon_2 * C_{we}.$$

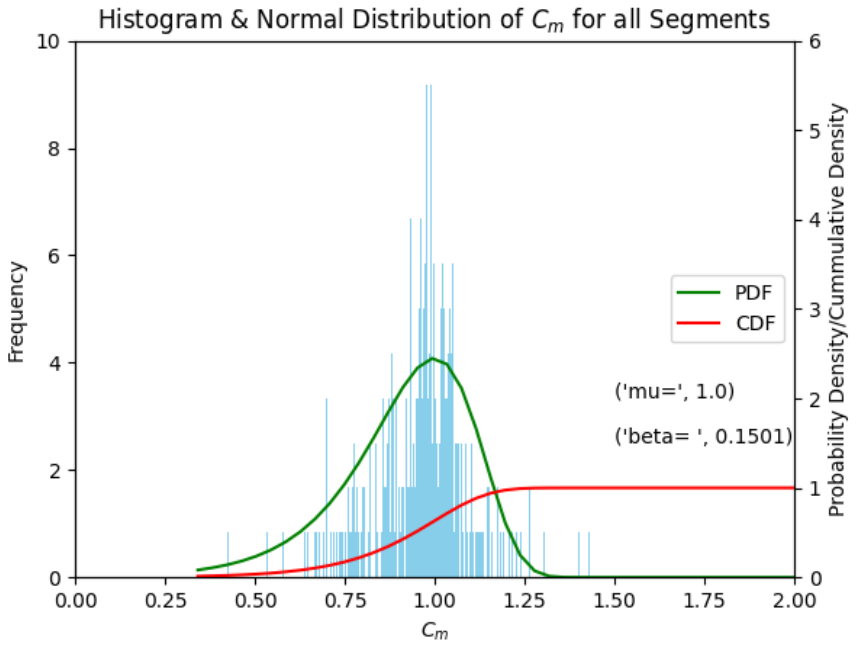

FIGURE 3-9 HISTOGRAM OF CM, THE FITTED APPROXIMATIONS OF LEFT-SKEWED GUMBEL PROBABILITY AND CUMULATIVE DISTRIBUTION FUNCTIONS.

A histogram for all values of C_m for all segments was similarly plotted, and the distribution approximated to a Gumbel distribution. A probability distribution curve and a cumulative distribution curve were superimposed on the histogram. The congestion contribution, R_c, is calculated using the cumulative distribution function $F_c(x)$, derived from the probability distribution function below.

$$f(x) = \frac{1}{\beta} * e^{\left(\frac{x-\mu}{\beta}\right)} * e^{-e^{\left(\frac{x-\mu}{\beta}\right)}}$$

$$R_c(C_m) = 1 - e^{-e^{\left(\frac{C_m-\mu}{\beta}\right)}}$$

Where μ and β are the location and scale parameters respectively. In figure 3-9 above they are presented as *mu* and *beta*.

Bottleneck Ranking

The bottleneck ranking is a probe data analytics tool that ranks congestion along TMC segments over an extended period. The ranking was obtained as a file separate from the Readings file and it contained only the worst 1000 segments in Tennessee. The severity of bottlenecking increased as the numerical positions decreased to zero. The primary loop initialized in the planning time index section above also opened, read, and wrote the bottleneck ranking file columns into lists, and the column headers removed. Each loop iteration scanned the bottlenecking list containing the segment codes to find a match. When the segment was found, its index was incremented by 1 to indicate its position, n_b. Otherwise, n_b is zeroed. The bottleneck contribution of a TMC segment, R_b, is given by

$$R_b = \frac{n_b}{1000}$$

All TMC segments with a zero value for n_b and the segment ranked 1000 in the bottleneck ranking file receive R_b value of 1.

Development of Database and Webserver

In addition to traffic signal rankings, an on-line database was built to be accessed from the Internet. The database was built in the *Xampp* environment which enabled access to the ranking results over a web browser. In what follows, the details of database development and webserver construction will be discussed.

Database

Amazon Web Services Elastic Cloud 2 (EC2) instances provide invaluable testing and development environments for remote computing with variable processing capacity, and web server hosting. One such instance was used in this study to develop a web database through which the intersection ranking results can be accessed online. In the instance, a MySQL database was created to host a table with the identifying information of all the intersections extracted, as well as the ranking information. The table consolidated data from the TMC Identification file and the calculated rankings, into columns that were classified as three categories:

- Front-end identifiers including road names, county, segment end latitude and longitude coordinates, and zip code.
- Back-end identifiers including id column set as the primary key, segment codes.
- Ranking information including overall ranking, average aggregate congestion, and average planning time index.

A python script was used to write the intersection ranking information to the database table using the MySQL Connector library. The end latitude and longitude coordinate columns were fused into one column, *GPS coordinates*. This facilitated the geolocation

of the intersections using Google Maps links for each intersection. To make the database table visible via a web browser, the web development application *Xampp* was used.

Website

Xampp is embedded with a *MySQL* server and an Apache server. Both embedded servers are independent of the local Apache2 and MySQL servers that may be running in the host machine. Both sets of servers cannot be operational at the same time, so the local servers were turned off and the *Xampp* servers booted up. In a web browser in the host machine, a localhost connection was made accessible. The MySQL server was accessed through the *PhpMyAdmin* page on the localhost, and the database table created and populated as detailed in the subsection above. A *php* file was written and it read the database table and displayed its contents in a web browser. The file also read and converted the GPS coordinates column into Google Maps links such that each intersection can be shown by the coordinates at its center. More *php* code scripts were written for the search and sort functionalities of the list of intersections, using a mix of JavaScript and Ajax programming. The search prompt is active for all columns of the table, while the sort prompt rearranges the entire table using ascending or descending order based on one column. The website was initially made internally accessible to the City of Murfreesboro and City of Franklin traffic control agencies to assess the performance of their traffic signals. Per the request of TDOT and due to the high cost of hosting the website on Amazon EC2, the website has been taken down. Due to security concerns, the website was made maintained as an internal asset and the results are presented in a csv file in the appendix. The file is an export of the database table containing the ranking results.

Chapter 4 Results & Discussion

Ranking Formula

Using the final layout and configuration of the website, testing was conducted on the initial intersections to determine viability as mentioned earlier. The GPS coordinates column of the table linked each intersection to a GPS pin-drop on Google Maps. A viable intersection was determined using the following decision tree as shown in Figure 4-1 below:

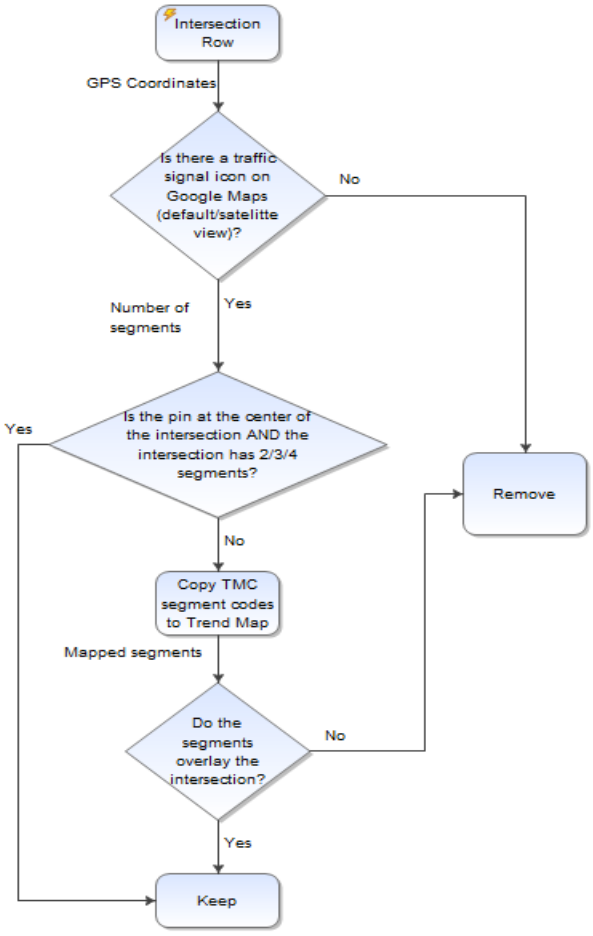

FIGURE 4-1 FLOW CHART FOR DETERMINATION OF INTERSECTION VIABILITY.

The intersections were initially deemed viable when the drop pin occurred at an area where Google Maps showed a small traffic signal icon. The intersection was then confirmed as viable if the pin was at the center of the intersection *and* it consisted of 2, 3 or 4 segments only. If more than 4 segments were involved, the segments were inserted into the Trend Map tool and mapped. If the mapped segments overlayed the intersection per the description in the python script, it was kept. Otherwise, the intersection would be removed. The list of intersections was finalized by compiling the intersections to be removed and using a python script to remove them from the database table connected to the website.

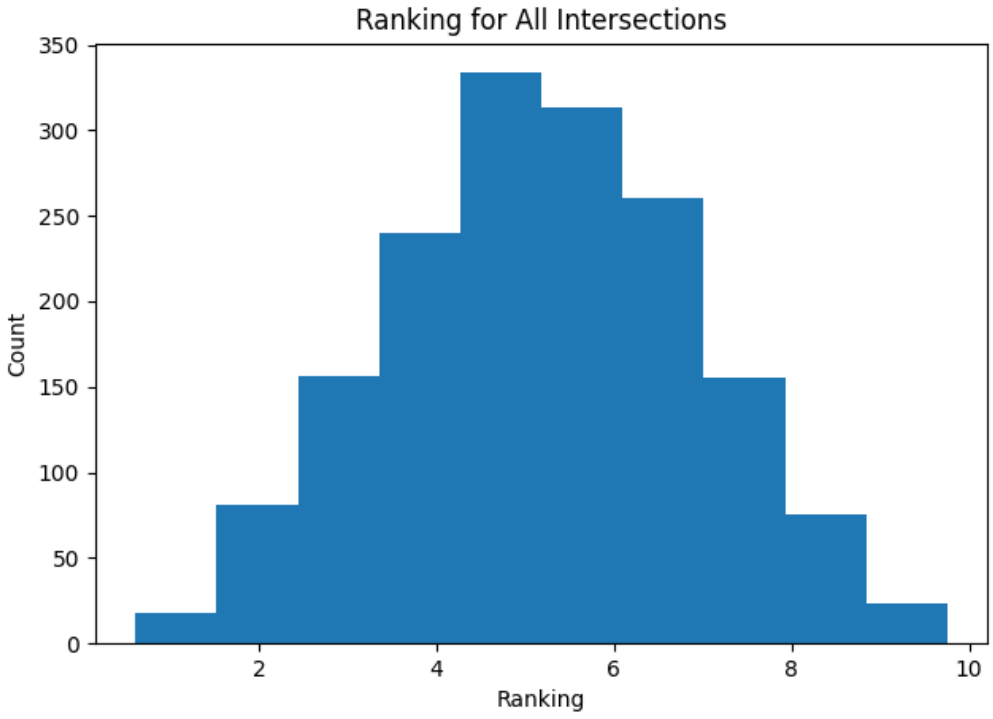

FIGURE 4-2 HISTOGRAM OF INTERSECTION RANKS SHOWING APPROXIMATELY NORMAL DISTRIBUTION.

Figure 4-2 shows the histogram of the traffic signal rankings, which is close to a normal distribution. The extreme left indicates that the poorly performing intersections had poor performance for each individual metric: an average congestion *significantly* below 1, an average planning time index *significantly* greater than 1, and a bottleneck ranking near the top of the list. These intersections were indicative of areas of near-constant heavy traffic including areas of business in downtown Nashville, Memphis, and Knoxville, and areas of periodic heavy traffic in the morning and evening time-of-day windows including areas surrounding educational establishments, K-12, and colleges/universities alike. On the other hand, the intersections at the other end of the spectrum were mostly located in areas with lesser densities of businesses and educational establishments. Some of these intersections are located along state highway routes which generally experience less congested traffic. The center of the histogram is a result of different combinations of $R_p, R_c, and\ R_b$. Since the bottleneck ranking (and its contribution R_b) is a cumulative for the entire dataset, congestion and PTI can be used to explain the combinations that heavily impact the rankings.

In the development of the metrics, each TMC segment's performance for the study period was measured up against its own best period (free flow speed and travel time). These measures, expressed as the ratios $R_p\ and\ R_c$, allowed the ranking formula to be uniformly applied across all segments without considering other factors including length of individual segment. In Figure 4-3, the vertical blue line is at average congestion value 1: all intersections occurring along this line have TMC segments on which the average speed was equal to the free flow speed. Conversely, the red horizontal line is at planning

time index value 1: all intersections on this line have segments on which a driver would not need to allocate any additional time for a worst-case travel time. An inverse correlation relationship is observed: the maximum planning time index decreases as the average congestion increases.

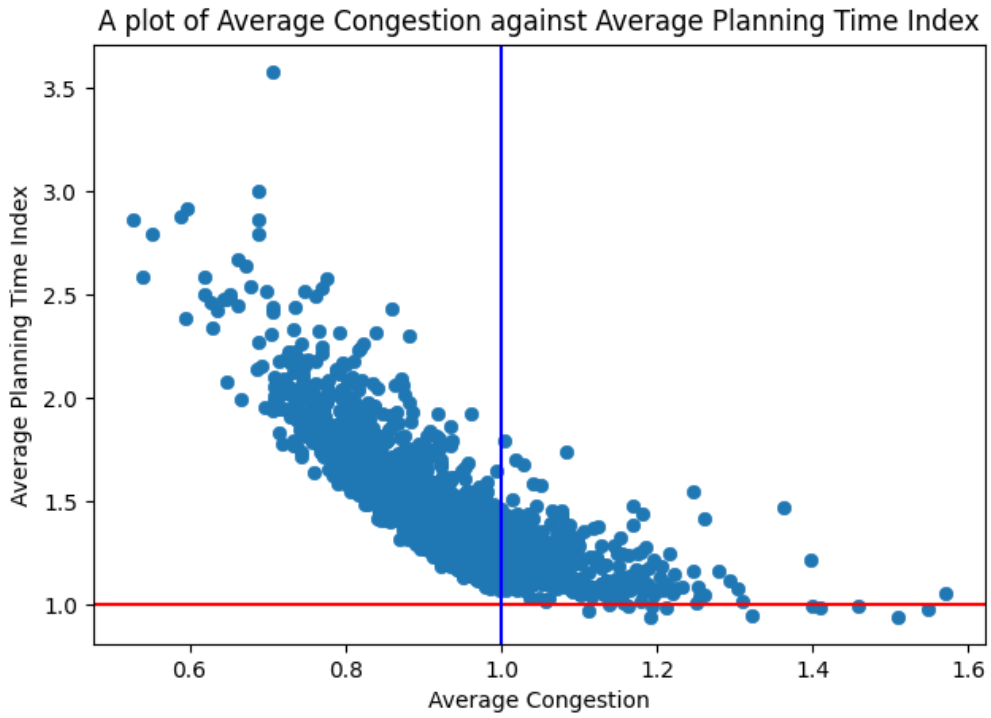

FIGURE 4-3 SCATTER PLOT OF AVERAGE CONGESTION AGAINST PLANNING TIME INDEX USING THE INITIAL 4/4/2 WEIGHT SPLITS, SHOWING A CORRELATION.

Since the planning time index and congestion are related due to the use of the common travel time, the following observations can be made if the blue and red lines divide the figure into four partitions:

i. Most intersections had average speeds below the free-flow speed and as such, had PTI values greater than 1 (upper left partition). The commuter would have to plan

extra time for worst-case scenario of their commute since they will be travelling at speeds below the free flow.

ii. Some intersections had average speeds greater than free flow, but the PTI was greater than 1 (upper right partition). Outlier instances of congestion increase the travel time, thus increasing the PTI.

iii. Even fewer intersections enjoyed uncongested travel throughout the month (bottom right quadrant). These intersections had average speeds greater than free flow and did not have a recorded instance of congestion in the selected time windows, which would have led to increases in travel time. These recorded travel times remained at/below free flow travel time.

iv. It was practically impossible to have any intersections represented in the bottom left quadrant. If the average speed is below the free flow speed, the commuter *must* plan additional time for the worst-case scenario.

The month of September 2021 was chosen due to its sheer volume of traffic. Traditionally, September brings about the end of the summer holidays and a return to school. In 2021, this was coupled with the return to in-person instruction for K-12 and colleges in Tennessee. Back to school shopping and transit to and from the educational facilities also drive a change in traffic patterns for surrounding areas. Capturing traffic data from the morning, midday and evening times of day encapsulates the peak volume of traffic especially during the weekdays. While the methodology in this study utilizes data from only this one month, it is intended to be used, irrespective of the month, to influence retiming decisions for transportation agencies throughout the year.

Comparison to Expert Rankings

The ranking formula results were compared with the LOS results provided by City of Murfreesboro and City of Franklin for a list of 54 selected signalized intersections in their cities. Figure 4.5 below shows the comparison result where [0,10] is divided into 6 intervals, corresponding to the 6 LOS letter grades. Among 17 traffic signals, there is a match between the ranking formula results and the LOS grades; the ranking formula results are better at only 7 intersections; for the rest of the traffic signals (30), the ranking formula results were harsher. After discussions with the traffic engineers at both cities, the discrepancy was determined to be due to the following three reasons:

i. The LOS grades of these intersections were solely determined by a single performance metric: the average control delay.
ii. The cities' data from some intersections was outdated, with some evaluations from as far back as 2015.
iii. The cities might not have collected the average control delay data from different times of the day and different days of the week from an entire month.

The ranking formula addresses all these issues in the quest to provide an evaluation that is recent and includes multiple measures for better understanding of signal performance.

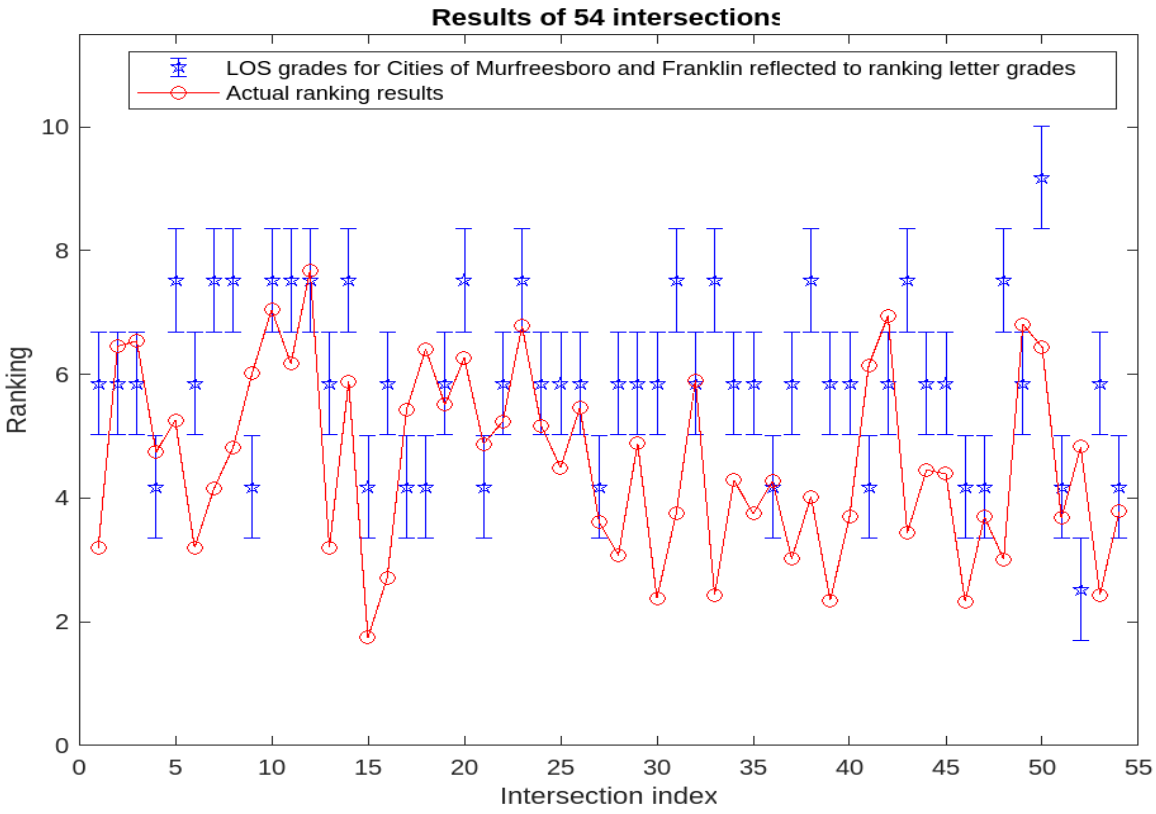

FIGURE 4-4 COMPARISON OF RANKING RESULTS WITH LEVEL OF SERVICEABILITY LETTER GRADES FROM LOCAL TRAFFIC JURISDICTIONS.

Chapter 5 Traffic Controller Experimentation & ATSPM Emulation

In this chapter, the general goal was to implement Automated Traffic Signal Performance Measures (ATSPM) using a simulated intersection complete with vehicle detection. An Econolite Cobalt traffic signal controller (Fig. 5.1) with built-in high-resolution data logging. Initial tests were conducted on the controller to determine how it carries out its functions.

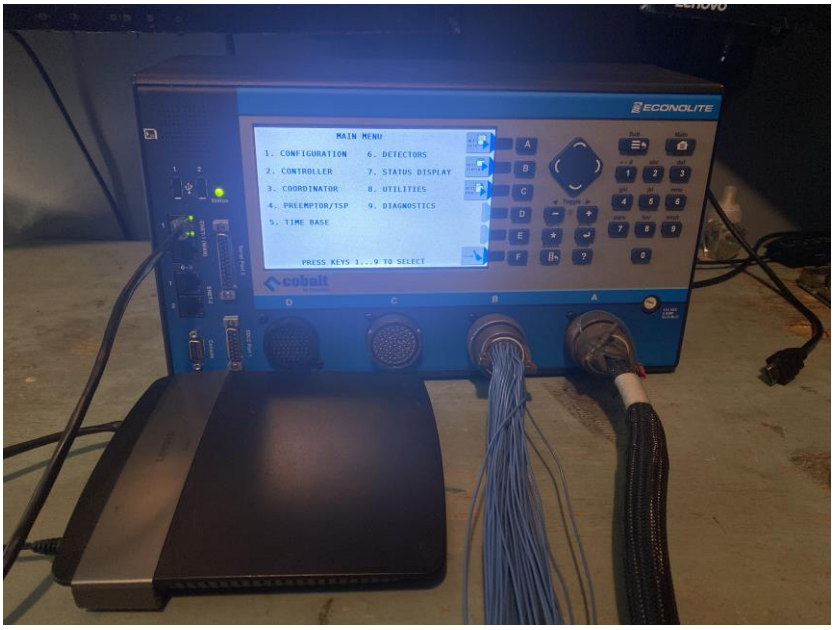

FIGURE 5-1 A CLOSE-UP OF THE ECONOLITE COBALT TRAFFIC SIGNAL CONTROLLER.

Controller Tests

Timing & Signal Lights

Timing sequences for the controller are input through the front panel graphical user interface. Durations for the green light for eight primary phases (4 through and 4 left turn phases) are entered along with other configurations to control the traffic signals. The front panel also contains four harness connections that lead to input/output pins (figure 5-3) from the controller through which it is connected to various field instruments including limit switches for the red/yellow/green lights, and detectors. The controller provides three output pins for each phase, one for each light to signal a specific direction of travel. These phase control pins are provided with a 24V vcc while the signal is not called: while the green light for phase two is off, 24V is provided through the pin for the phase two green. When the pin provides 0V (grounded), the green for phase two is active and cars can go through the intersection. A circuit using integrated circuit (IC) chips with logic gates (figure 5-2) was utilized to emulate this effect.

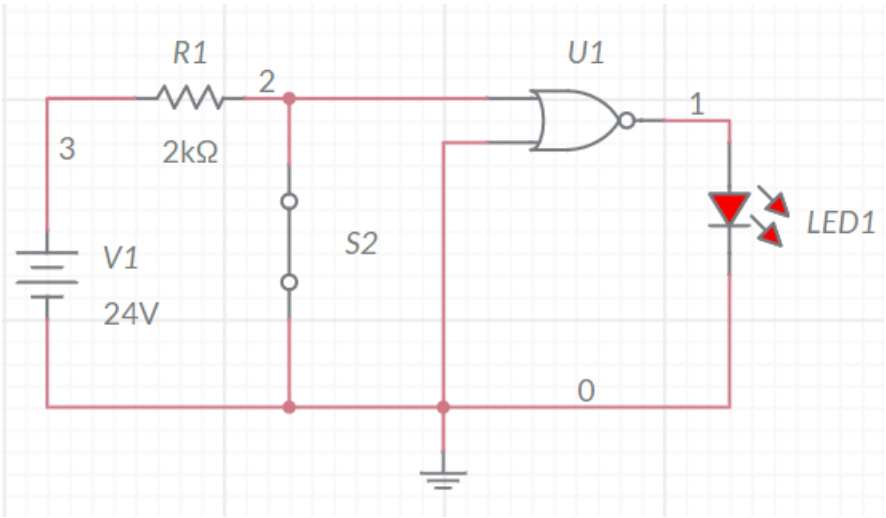

FIGURE 5-2 AN IC CIRCUIT USED WITH LOGIC GATES AND A 24V SOURCE.

Data Generation

Loop detector calls were emulated by using a switch to make and break the connection between the phase-specific input pins. Figure 5-3 below shows a snapshot of the table containing the pin layout for the controller. For example, Pins *K* and *L* in connectors A and B respectively are shown as detector pins. The controller provides a constant 24V at its detector pins. When these pins are connected to the ground through an external circuit, the detector registers a detector call. Another IC circuit (figure 5-4) was designed to emulate field detection. An Arduino was connected to provide the 5V at switch S1 which was toggled on/off to simulate passing cars activating a stationary detector.

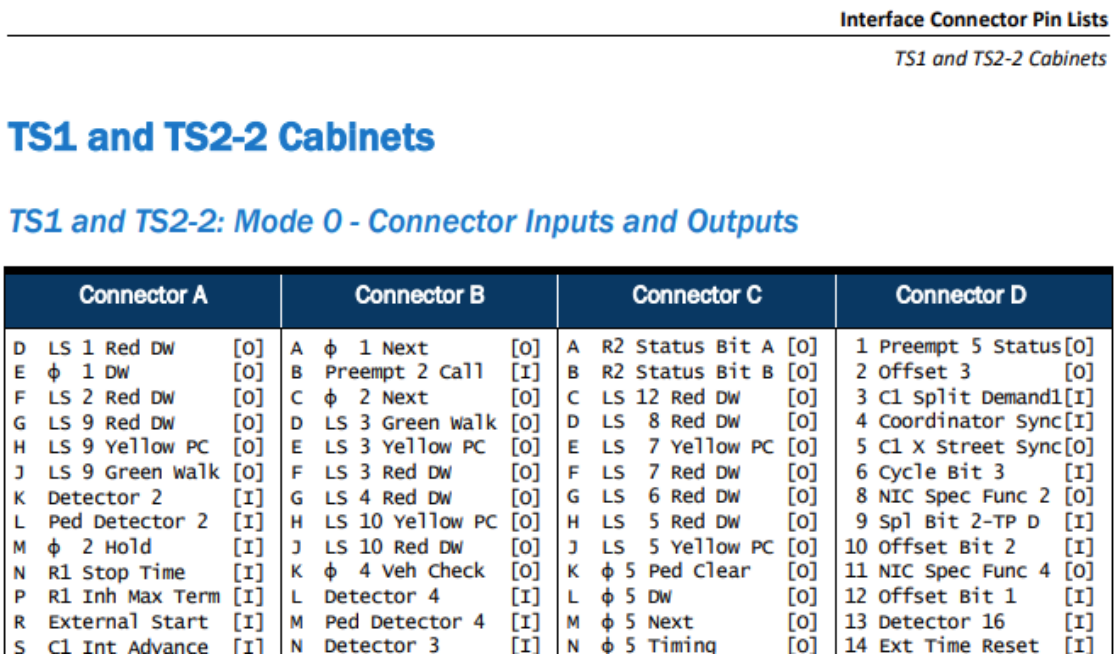

Interface Connector Pin Lists

TS1 and TS2-2 Cabinets

TS1 and TS2-2 Cabinets

TS1 and TS2-2: Mode 0 - Connector Inputs and Outputs

Connector A			Connector B			Connector C			Connector D		
D	LS 1 Red DW	[O]	A	ϕ 1 Next	[O]	A	R2 Status Bit A	[O]	1	Preempt 5 Status	[O]
E	ϕ 1 DW	[O]	B	Preempt 2 Call	[I]	B	R2 Status Bit B	[O]	2	Offset 3	[O]
F	LS 2 Red DW	[O]	C	ϕ 2 Next	[O]	C	LS 12 Red DW	[O]	3	C1 Split Demand1	[I]
G	LS 9 Red DW	[O]	D	LS 3 Green Walk	[O]	D	LS 8 Red DW	[O]	4	Coordinator Sync	[I]
H	LS 9 Yellow PC	[O]	E	LS 3 Yellow PC	[O]	E	LS 7 Yellow PC	[O]	5	C1 X Street Sync	[O]
J	LS 9 Green Walk	[O]	F	LS 3 Red DW	[O]	F	LS 7 Red DW	[O]	6	Cycle Bit 3	[I]
K	Detector 2	[I]	G	LS 4 Red DW	[O]	G	LS 6 Red DW	[O]	8	NIC Spec Func 2	[O]
L	Ped Detector 2	[I]	H	LS 10 Yellow PC	[O]	H	LS 5 Red DW	[O]	9	Spl Bit 2-TP D	[I]
M	ϕ 2 Hold	[I]	J	LS 10 Red DW	[O]	J	LS 5 Yellow PC	[O]	10	Offset Bit 2	[I]
N	R1 Stop Time	[I]	K	ϕ 4 Veh Check	[O]	K	ϕ 5 Ped Clear	[O]	11	NIC Spec Func 4	[O]
P	R1 Inh Max Term	[I]	L	Detector 4	[I]	L	ϕ 5 DW	[O]	12	Offset Bit 1	[I]
R	External Start	[I]	M	Ped Detector 4	[I]	M	ϕ 5 Next	[O]	13	Detector 16	[I]
S	C1 Int Advance	[I]	N	Detector 3	[I]	N	ϕ 5 Timing	[O]	14	Ext Time Reset	[I]

FIGURE 5-3 A SNAPSHOT OF THE PIN LAYOUT FOR THE COBALT CONTROLLER.

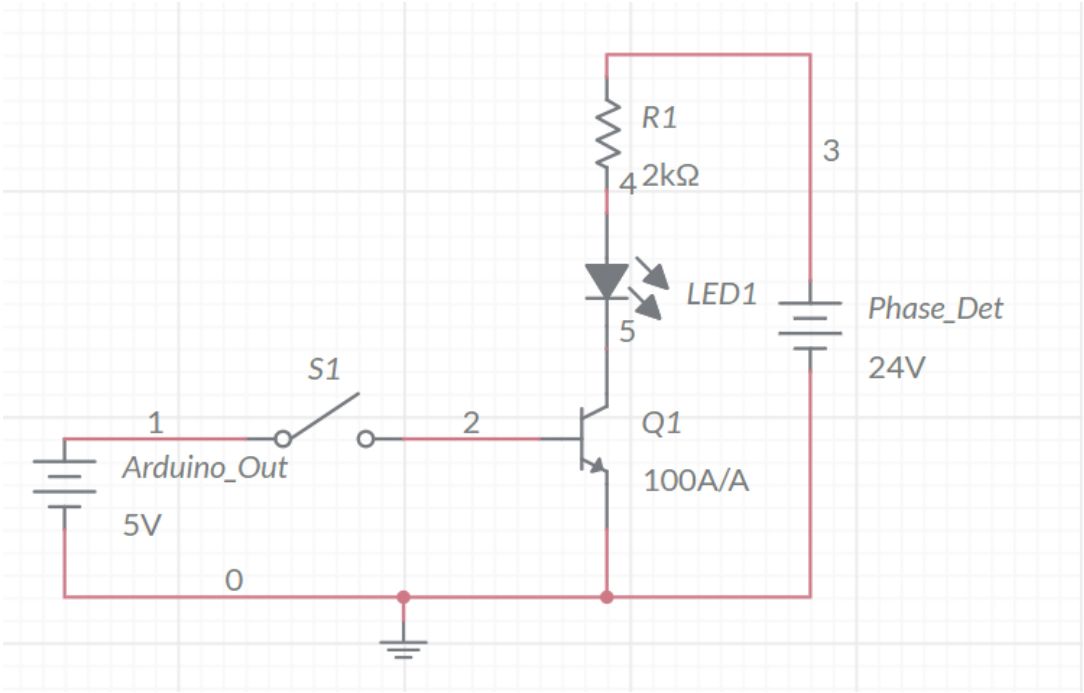

FIGURE 5-4 A SIMPLE IC CIRCUIT TO EMULATE DETECTION.

Networking

The networking capability was tested using a wireless router and a PC. The signal controller was connected to the router via Ethernet cable, and the PC was connected to the router's Wi-Fi network. In the controller's Ethernet settings, the IP address was configured to match the subnet of the router so that all devices are on the same network. Using a Windows PC's command window, the IP address of the controller was pinged with a low round-trip response time, showing that the network connection was solid (see Figure 5-5).

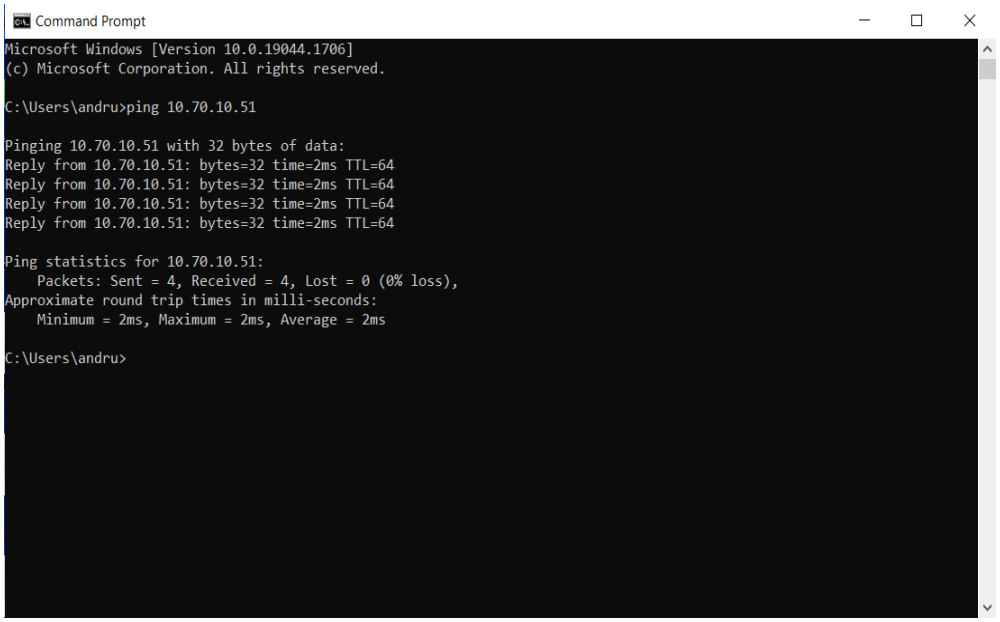

FIGURE 5-5 A SNAPSHOT OF THE WINDOWS COMMAND PROMPT SHOWING AN AVERAGE OF 2MS PING RESPONSE TIME.

Web Interface

The controller was also accessed through the web front panel, using the configured IP address and port 8081. From the web interface, changes can be made to controller configurations and signal timings (see Figure 5-6 for the web front panel).

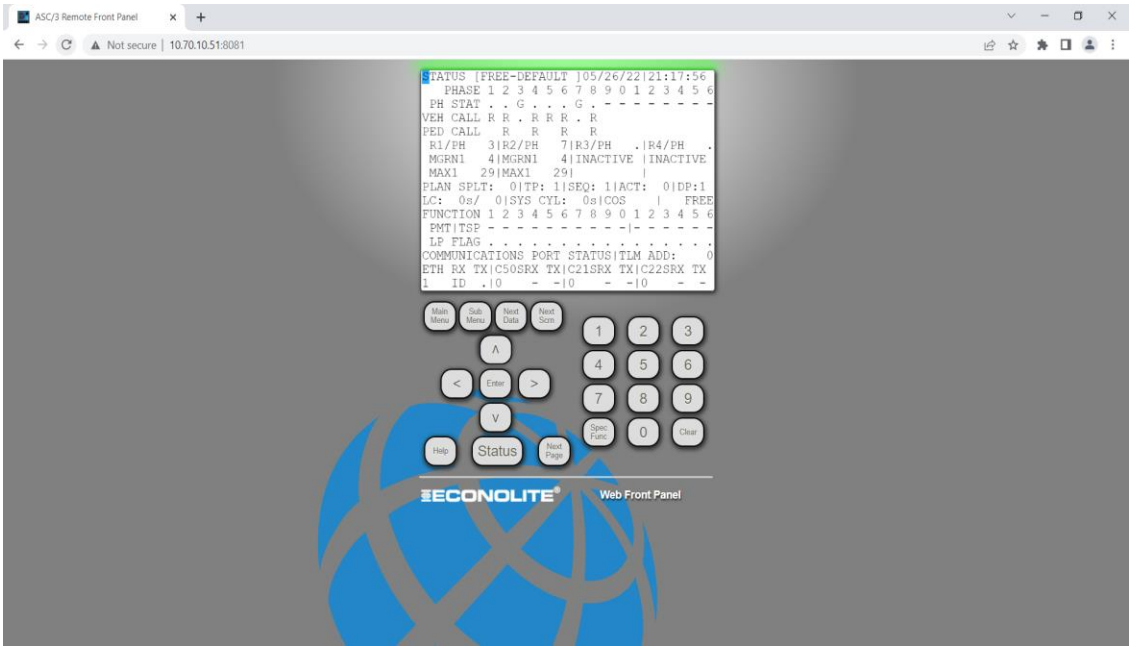

FIGURE 5-6 SNAPSHOT OF A WEB BROWSER SHOWING THE CONTROLLER WEB FRONT PANEL.

Data Logging and File Transfer

To configure the controller for ATSPM, hi-resolution data logging must be enabled in the settings. The log files that contain events at the intersection can be stored at 1-minute, 15-minute, or 1-hour intervals. Figure 5-7 shows the Web Front Panel with the interval set at 15 minutes (right middle), which is most used with ATSPM applications. The log files are located on the controller, in its *set1* directory as shown in Figure 5-8 below where the *WinSCP* SSH File Transfer Protocol software on a PC was used to connect to the controller. The *.datz* files in the set1 directory were translated through proprietary software provided by Econolite tech support to glean valuable information from the logs. Figures 5-9 and 5-10 show the detector events section of the Purdue phase enumerations [28], and the translated csv file containing timestamped logs with the phase enumeration codes respectively.

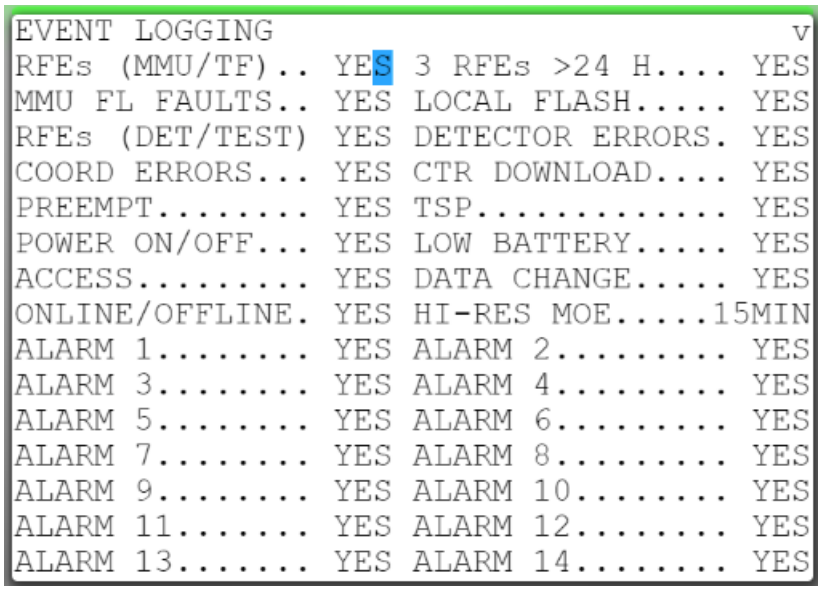

FIGURE 5-7 SNAPSHOT OF THE WEB FRONT PANEL SHOWING THE EVENT LOGGING MENU WITH "HI-RESOLUTION MOE" LOGGING TURNED ON.

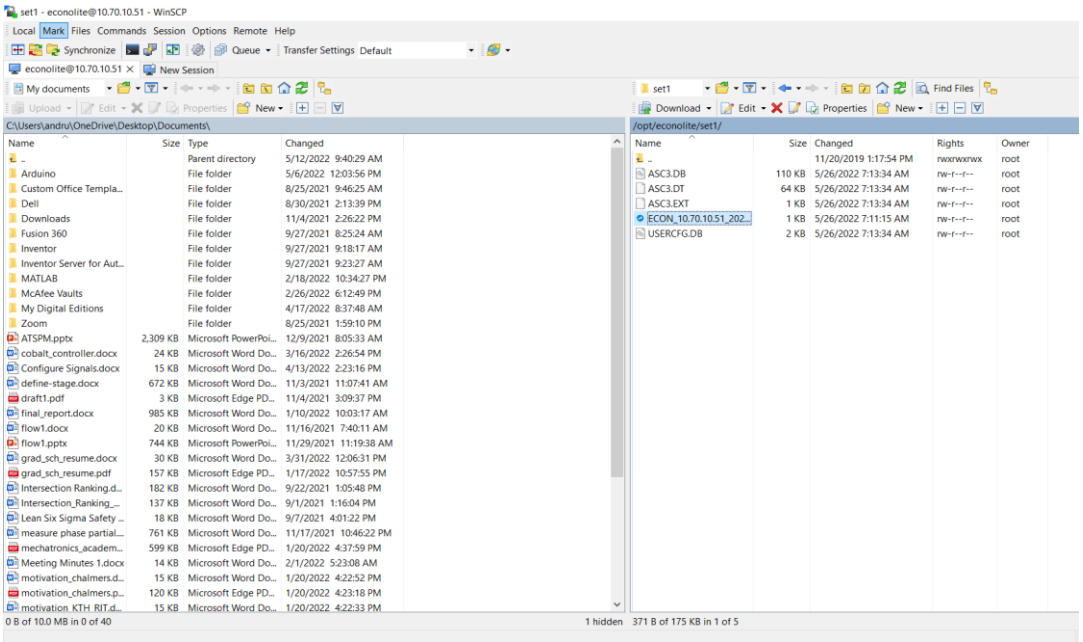

FIGURE 5-8 A SNAPSHOT OF THE WINSCP WINDOW SHOWING TRAFFIC LOG FILES ON THE RIGHT.

Detector Events:			
81	Detector Off	DET Channel # (1-64)	Detector on and off events shall be triggered post any detector delay/extension processing.
82	Detector On	DET Channel # (1-64)	
83	Detector Restored	DET Channel # (1-64)	Detector restored to non-failed state by either manual restoration or re-enabling via continued diagnostics.
84	Detector Fault- Other	DET Channel # (1-64)	Detector failure logged upon local controller diagnostics only (not system diagnostics).
85	Detector Fault- Watchdog Fault	DET Channel # (1-64)	Detector failure logged upon local controller diagnostics only (not system diagnostics).
86	Detector Fault- Open Loop Fault	DET Channel # (1-64)	Detector failure logged upon local controller diagnostics only (not system diagnostics).
87	Detector Fault- Shorted Loop Fault	DET Channel # (1-64)	Detector failure logged upon local controller diagnostics only (not system diagnostics).
88	Detector Fault- Excessive Change Fault	DET Channel # (1-64)	Detector failure logged upon local controller diagnostics only (not system diagnostics).
89	PedDetector Off	DET Channel # (1-16)	Ped detector events shall be triggered post any detector delay/extension processing and may be set multiple times for a single pedestrian call. (with future intent to eventually support ped presence and volume)
90	PedDetector On	DET Channel # (1-16)	
91	Pedestrian Detector Failed	Ped Det # (1-16)	Detector failure logged upon local controller diagnostics only (not system diagnostics).

FIGURE 5-9 SNAPSHOT OF THE PURDUE PHASE ENUMERATIONS SHOWING THE DETECTOR CODES.

	A	B	C	D	E	F	G	H	I	J	K
1	Timestamp	Event Type	Parameter								
2	50:00.0		Version #	3							
3	50:00.0		ECON_10.70.10.51_2022_07_19_1150.dat								
4	50:00.0		Intersection #	10.70.10.51							
5	50:00.0		IP Address:	10.70.10.51							
6	50:00.0		MAC Address:	00:04:81:06:4f:b1							
7	50:00.0		Controller Data Log Beginning:	50:00.0							
8	50:00.0		Phases in use:	1	2	3	4	5	6	7	8
9	50:00.1	81	4								
10	50:01.5	82	4								
11	50:01.8	81	4								
12	50:03.0	23	2								
13	50:03.0	23	6								
14	50:03.2	82	4								
15	50:03.6	81	4								
16	50:04.9	82	4								
17	50:05.3	81	4								

FIGURE 5-10 SNAPSHOT OF THE TRANSLATED FILE LOG FILE SHOWING DETECTOR TOGGLING FOR PHASE 4.

ATSPM Experimentation

For the last section of the project, the ATSPM system was emulated using the information detailed in this chapter and a widely available installation manual. The controller setup detailed earlier in this chapter was utilized to emulate a field intersection. Following relevant networking and security configurations, the website and webserver were set up to receive data from this one signal and display it at (post site link). The configuration files (ATSPM Files) set up the relevant protocols [29] to get the data from the controller logs to the online server, translate it to performance measures which are then displayed on the web user interface. The website provided configuration options for the intersection, which was modeled after the Middle Tennessee Blvd. and E Main St. intersection in Murfreesboro. The configurations include adding phases and directions of travel, as well as various phase-specific detectors (see figure 5-11). These settings must match the configurations of the phases and detection on the controller for the data displayed on the website to accurately present the traffic conditions. The configurations on the controller can be found in the config file attached in the appendix.

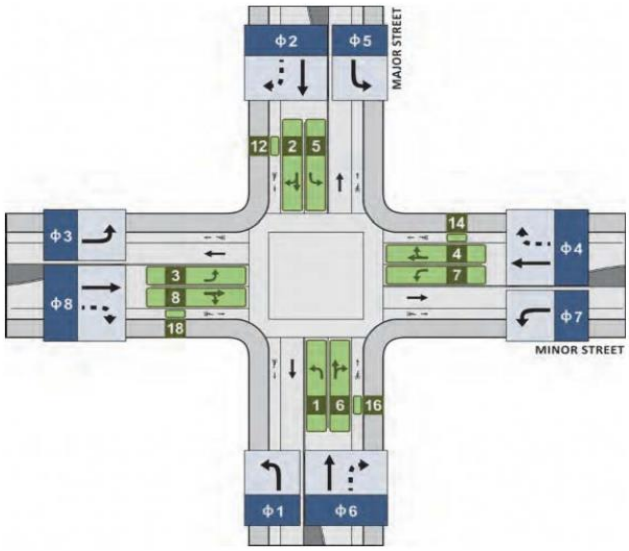

FIGURE 5-11 A SAMPLE INTERSECTION SHOWING EIGHT PRIMARY PHASES OF TRAFFIC AND THEIR DIRECTIONS.

The controller was then connected to all the components mentioned above in this chapter thus simulating an intersection. An Arduino was used to control the base nodes of the transistors used for detection (figure 5-4) as shown in the appendix. The code was used to dictate the volume of traffic in the through phases. Queue lengths of 5-15 cars per cycle were used to signify light traffic and 15-25 for heavier traffic. It should be noted that this code simulates a specific scenario of traffic where all cars that pass the advance detector (set 350 feet from the stop bar at the intersection) must also pass the stop bar detector. It was assumed that some cars peel off for the left and right turns, and an equal number of cars join the queue from side streets. This scenario was adequate to execute through the simulations. The figures 5-12, 13 & 14 below show charts of measures provided by the website for phase 4: the lighter traffic was observed between 11:15-11:30 pm while the heavier traffic was observed from 11:30pm-12:00am.

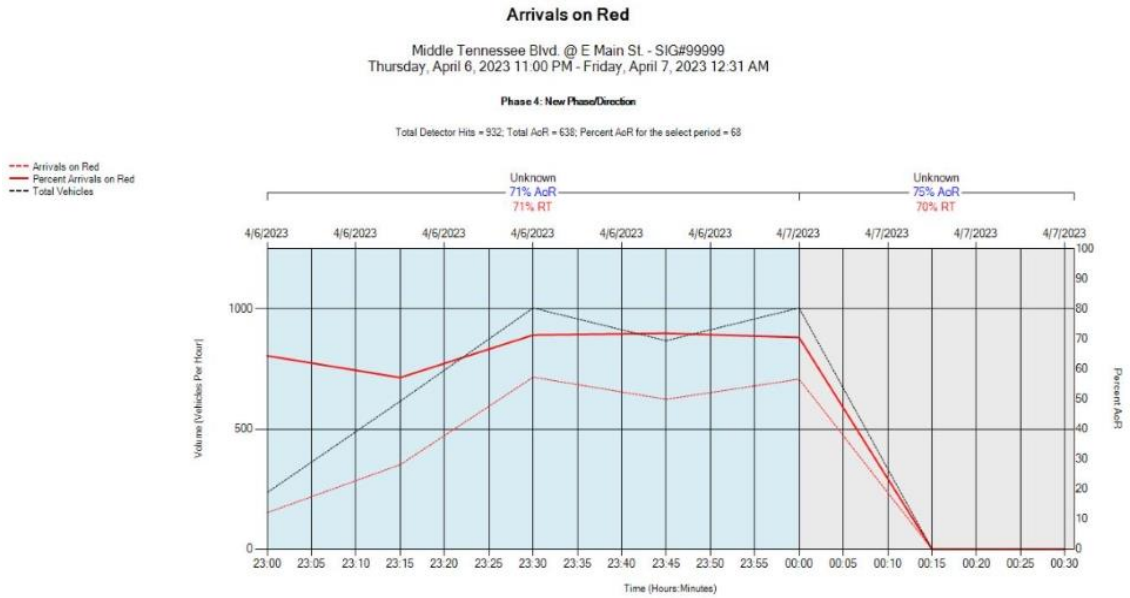

FIGURE 5-12 A CHART SHOWING THE ARRIVALS ON RED FOR PHASE 4.

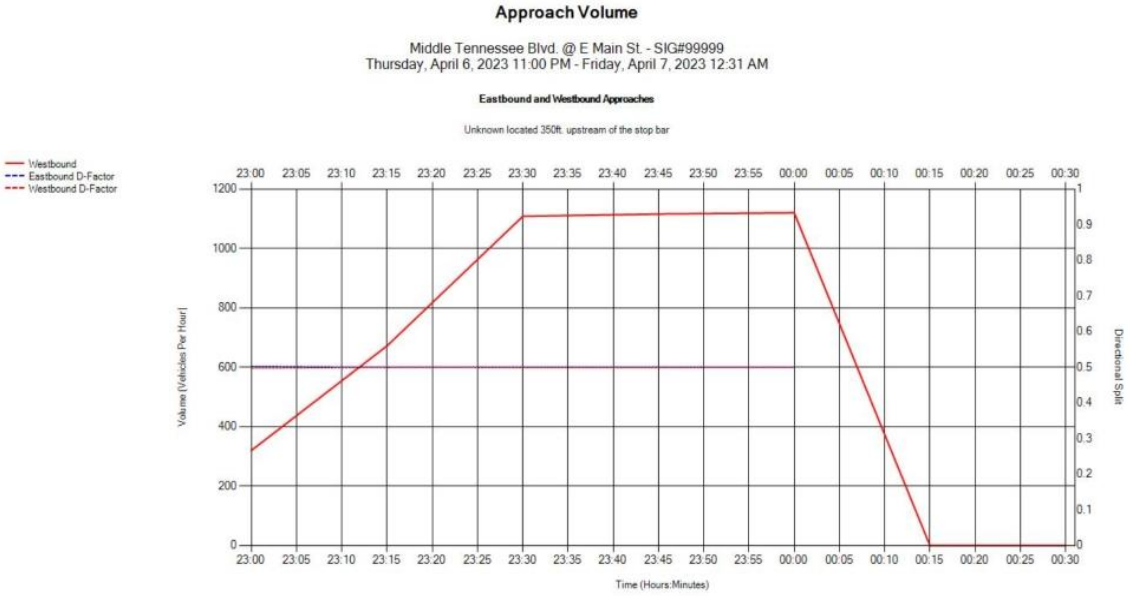

FIGURE 5-13 A CHART SHOWING THE APPROACH VOLUME FOR PHASE 4.

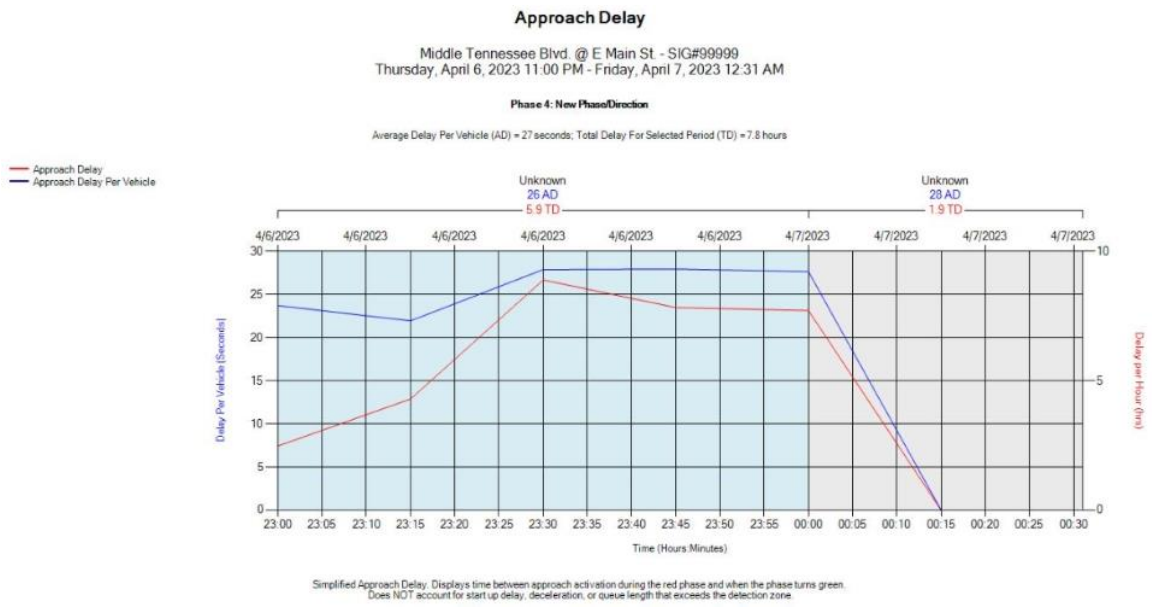

FIGURE 5-14 A CHART SHOWING THE APPROACH DELAY FOR PHASE 4.

The arrival on red measure refers to the number of vehicles that arrive during the red cycle. Conversely, the arrival on green refers to the number of vehicles that arrive during the green cycle. These two measures together can be used to measure vehicle delays [16]. The approach volume is the number of vehicles arriving at the intersection and it is divided into the configured directions of travel.

Since arrivals on red, approach volume and approach delay are directly related to the number of cars and what cycle of traffic they are detected, the average increases observed in all three charts from 23:15-23:30 to 23:30-00:00 can be directly attributed to the increase in the queue lengths implemented in the Arduino code. Unfortunately, due to cost handicaps, additional hardware could not be acquired to configure the collection of speed data.

Chapter 6 Conclusions

In this project, an online traffic signal ranking database with 1655 traffic signals in Tennessee was implemented using data from TMC segments. Three metrics were developed to evaluate the performance of the individual segments during September 2021 with respect to each segment's best (free flow) performance. Each segment was evaluated on congestion, planning time index, and bottleneck ranking, and a formula provided a numeric rank from 0-10. The intersection ranks were determined as the average of the ranks for each inbound segment at an intersection. These rankings served as a performance evaluation of the traffic signals and can be utilized to prioritize retiming for local and regional traffic agencies. While the implementation of comprehensive traffic evaluation systems like the ATSPM has gradually increased, the methodology implemented in this project can serve as a screening tool to pinpoint specific problem intersections where more in-depth data should be collected for retiming.

An online database was implemented to record the ranking results and provide web browser connectivity for traffic agencies in Tennessee. The website contained the ranking information as well as the signal identifying information which the agencies can use in prioritization of signals for retiming. Signals in each agency's jurisdiction can be viewed using the search and sort operations of the website. The ranking formula and the website will also be great tools to researchers looking at alternate ways of traffic signal evaluation, and the public curious about signal performance.

The ranking formula results were compared with the LOS letter grades of 54 intersections in the Cities of Murfreesboro and Franklin. The formula provided mostly harsher

evaluation than the LOS letter grades, which only relied on the average control delay metric. Some of the expert data was outdated, with evaluations from as far back as 2015.

Further research will benefit from the improvement of the TMC segmentation to increase the coverage and clarify the segment breaks. More roads would be included in the segmentation and intersections could be more clearly defined. An added advantage would be achieved if signalized intersections were distinguished from others. While this study utilized historical data (after the month of September 2021 concluded), it could benefit local agencies to use more recent data which would require more data storage and processing capacity. Additional studies could benefit from using more performance metrics including accident and safety measures.

The controller testing and simulation of an intersection for ATSPM provided invaluable insight on how the controller carries out its functions. Much of the knowledge gained in this portion of the research was tribal in nature and was gained through constant dialogue with experts for both controller and website/server. The work documented in chapter 5 adds to the body of knowledge for how a signaled intersection carries out its functions through the controller, and the depth of data that can be collected from activity at the intersection. It will prove to be a valuable resource for researchers carrying out studies on signal performance with limited field equipment.

References

[1] D. Schrank, T. Lomax, B. Eisele, 2012 Urban Mobility Report, Tech. rep.,Texas A&M Transportation Institute Mobility Division (2012).

[2] D. Schrank, L. Albert, B. Eisele, T. Lomax, 2021 Urban Mobility Report, Tech. rep., Texas A&M Transportation Institute Mobility Division (2021).

[3] Fast facts: U.S. Transportation Sector Greenhouse Emissions, Office of Transportation and Air Quality (2021).

[4] D. Metz, Economic benefits of road widening: Discrepancy between outturn and forecast, Transportation research part A: policy and practice 147 (2021) 312–319.

[5] A. Downs, The law of peak-hour expressway congestion, Traffic Quarterly 16 (3) (1962).

[6] G. Duranton, M. A. Turner, The fundamental law of road congestion: Evidence from U.S. cities, American Economic Review 101 (6) (2011) 2616– 2652.

[7] K. Hymel, If you build it, they will drive: Measuring induced demand for vehicle travel in urban areas, Transport policy 76 (2019) 57–66.

[8] C. Winston, A. Langer, The effect of government highway spending on road users' congestion costs, Journal of urban Economics 60 (3) (2006) 463–483.

[9] F. Romero, J. Gomez, A. Paez, J. M. Vassallo, Toll roads vs. public transportation: A study on the acceptance of congestion-calming measures in Madrid, Transportation Research Part A: Policy and Practice 142 (2020) 319–342.

[10] M. Börjesson, I. Kristoffersson, The swedish congestion charges: Ten years on, Transportation Research Part A: Policy and Practice 107 (2018) 35–51.

[11] H. Lu, S. Hess, A. Daly, C. Rohr, B. Patruni, G. Vuk, Using state-of-the-art models in applied work: Travellers willingness to pay for a toll tunnel in Copenhagen, Transportation Research Part A: Policy and Practice 154 (2021) 37–52.

[12] X. Wang, D. A. Rodríguez, A. Mahendra, Support for market-based and command-and-control congestion relief policies in Latin American cities: Effects of mobility, environmental health, and city-level factors, Transportation Research Part A: Policy and Practice 146 (2021) 91–108.

[13] P. Koonce, L. Rodegerdts, Traffic signal timing manual., Tech. rep., United States. Federal Highway Administration (2008).

[14] R. L. Gordon, Traffic Signal Retiming Practices in the United States, Vol. 409, Transportation Research Board of the National Academies of Sciences, Engineering and Medicine, (2010).

[15] G. Pacal, V. P. Sisiopiku, M. Hadi, Traffic signal operation, optimization, maintenance and management practices in the Southeast US, Traffic 16 (7) (2020) 08–18.

[16] Leitner, Dallas, Piro Meleby, and Lei Miao. "Recent advances in traffic signal performance evaluation." Journal of traffic and transportation engineering (English edition) (2022).

[17] S.M. Remias, A. M. Hainen, C. M. Day, T. M. Brennan Jr, H. Li, E. Rivera-Hernandez, J. R. Sturdevant, S. E. Young, D. M. Bullock, Performance characterization of arterial traffic flow with probe vehicle data, Transportation research record 2380 (1) (2013) 10–21.

[18] Z. H. Khattak, M. J. Magalotti, M. D. Fontaine, Operational performance evaluation of adaptive traffic control systems: A bayesian modeling approach using real-world gps and private sector probe data, Journal of Intelligent Transportation Systems 24 (2) (2020) 156–170.

[19] C. M. Day, S. M. Remias, H. Li, M. M. Mekker, M. L. McNamara, E. D. Cox, D. M. Bullock, Performance ranking of arterial corridors using travel time and travel time reliability metrics, Transportation Research Record 2487 (1) (2015) 44–54.

[20] M. R. Dunn, H. W. Ross, C. Baumanis, J. Wall, J. Lammert, J. Duthie, N. Ruiz Juri, R. B. Machemehl, Data-driven methodology for prioritizing traffic signal retiming operations, Transportation Research Record 2673 (6) (2019) 104–113.
[21] A. Meijer, B. van Arem, M. Salomons, N. Cohn, P. Krootjes, Probe data from consumer gps navigation devices for the analysis of controlled intersections, in: ITS America 22nd Annual Meeting & Exposition (Washington DC), (2012).
[22] G. Wünsch, F. Bölling, A. von Dobschütz, P. Mieth, Bavarian Road Administration's use of probe data for large-scale traffic signal evaluation support, Transportation Research Record 2487 (1) (2015) 88–95.
[23] M. J. Kulathintekizhakethil, Transportation system performance measures using internet of things data, Ph.D. thesis, Purdue University (2018).
[24] C. W. Cheng, Developing a set of holistic signal retiming performance metrics: an evaluation of signal retiming efforts in Austin, Master's thesis, The University of Texas at Austin (2020).
[25] A. Sharma, N. Hawkins, J. G. Shaw, S. Knickerbocker, S. Poddar, et al., Performance-Based Operations Assessment of Adaptive Control Implementation in Des Moines, Iowa, Tech. rep., Iowa State University. Institute for Transportation (2018).
[26] Brenna, T. M., & Venigalla, M. M., Baseline arterial performance evaluation and signal system management by fusing high-resolution data from traffic signal systems and probe vehicles. In 2020 Forum on Integrated and Sustainable Transportation Systems (FISTS) (pp. 378-385). IEEE.
[27] C. Winfrey, P. Meleby, and L. Miao, "Using Big Data and Machine Learning to Rank Traffic Signals in Tennessee", Journal of Traffic and Transportation Engineering, 2023, accepted.
[28] Sturdevant, James R., Timothy Overman, Eric Raamot, Ray Deer, Dave Miller, Darcy M. Bullock, Christopher M. Day et al. Indiana traffic signal hi resolution data logger enumerations. (2012).
[29] Atkins North America. Georgia Department of Transportation: Automated Traffic Signal Performance Measures Installation Manual. (2019).

Appendix

The MDD files and the python scripts used to achieve the results detailed in this report are accessible at TDOT Traffic Signal Research.